1-1-2007

Determining thermal conductivity and absorption coefficient of semi-transparent liquids using numerical and experimental approach

Jayant Prabhakar Patil
University of Nevada, Las Vegas

NOTE TO USERS

DETERMINING THERMAL CONDUCTIVITY AND ABSORPTION COEFFICIENT OF SEMI-TRANSPARENT LIQUIDS USING NUMERICAL AND EXPERIMENTAL APPROACH

by

Jayant Prabhakar Patil

Bachelor of Engineering
Amravati University, India
2002

A thesis submitted in partial fulfillment
of the requirements for the

Master of Science Degree in Mechanical Engineering
Department of Mechanical Engineering
Howard R. Hughes College of Engineering

Graduate College
University of Nevada, Las Vegas
December 2007

UNLV
UNIVERSITY OF NEVADA LAS VEGAS
UNLV

Thesis Approval

The Graduate College
University of Nevada, Las Vegas

August 09, 2007

The Thesis prepared by

Jayant Prabhakar Patil

Entitled

Determining Thermal Conductivity and Absorption Coefficient of Semi-transparent Liquids Using Both Numerical and Experimental Approach

is approved in partial fulfillment of the requirements for the degree of

Master of Science in Mechanical Engineering

Examination Committee Chair

Dean of the Graduate College

Examination Committee Member

Examination Committee Member

Graduate College Faculty Representative

ABSTRACT

Determining the Thermal Conductivity and Absorption Coefficient of Semi Transparent Liquids Using both Numerical and Experimental Approach

by

Jayant Prabhakar Patil

Dr. Samir Moujaes, Examination Committee Chair
Professor of Mechanical Engineering
University of Nevada, Las Vegas

Thermal properties of the molten salts are emerging as one of the important areas of research. The motivation for this particular research originated from the use of molten salts in high temperature heat exchangers. The molten salts are transparent liquids at their melting point. Considering this aspect of molten salt which resembles with water the research is conducted on water and glycerin. The effect of radiation along with conduction is studied in calculating the thermal conductivity of water.

The effect of radiation on thermal conductivity is calculated using Rosseland's approximation method. Thermal conductivity is calculated as function of temperature. Different radiation sources are used in the experiment to investigate the overall dependence of thermal conductivity on temperature for water, glycerin and glycol

TABLE OF CONTENTS

LIST OF FIGURES

ACKNOWLEDGEMENTS

I would like to acknowledge the help and esteemed guidance of the Project Investigator and my academic advisor Dr. Samir Moujaes for providing supervision and assistance with every step of the work.

I would like to thank Dr. Anthony Hechanova, Dr. Mohamed Trabia and Dr. Mohamed Kaseko for their support.

I would like to thank the Department of Mechanical Engineering for funding the project.

Support from the Jeff Markle is greatly appreciated.

CHAPTER 1

INTRODUCTION

1.1 Abstract

Molten salts are emerging as one of the important materials for use in high temperature hydrogen production using nuclear energy as the energy source. These have a lot of promise because the heat transfer can be achieved with these molten salts with a pressure operation very close to atmospheric as these salts have a very high boiling point temperature. The thermal properties of some of these materials have not been accurately determined especially thermal conductivity. Some of these molten salts like Flinak have been propose for use as a heat transfer fluid in the intermediate heat exchanger (IHX) which transfers the heat from the nuclear cycle to the hydrogen production plant.. The molten salts are semi-transparent liquids indicating that heat flow through them is usually achieved by radiation and conduction if the fluid is quiescent. To try to address this technical issue three candidate fluids (Water, Glycol and Glycerin) that resemble molten salts behavior have been used to demonstrate the use of an experimental based techniques which offers the possibility of separately calculating the radiation absorption coefficient and the thermal conductivity for these fluids at a variety of mean operating temperatures. The approach eventually uses an approximate equation that is based on an energy balance through a thin axial slice of the fluid exposed to heat transfer from above. The equation is then used to determine through optimization techniques what are the best values of the

radiation coefficient and the thermal conductivity at a certain mean temperature. The thermal conductivity for that molten salt can then be used for typical heat duty calculations for the IHX operation. Issues of materials for high temperature and corrosivity applications need to be addressed before the method can be applied for these high temperature molten salts applications.

1.2 Literature Review

Over the last few years a vast amount of research has been conducted in the field of thermal conductivity measurement for transparent fluids. Some oft the researchers have made significant changes in the existing methods to determine the thermal conductivity of water. The transient hot wire method of measuring the liquid thermal conductivity has been modified (Trump and Luebke [5]) to provide the simplified operation through direct plotting of wire resistance as a function of logarithm of time. An electronic transient recorder operating from a logarithmic time base stores resistance readings at equal increments of log time. The inverse slope of the resulting curve is multiplied by the instrument constant which gives the thermal conductivity. The researchers tested this method on water and methanol. A new correlation for thermal conductivity of liquids is proposed by (Lei, Hou and Lin [16]). The proposed model is based on the fact that the liquid is composed of a mixture of micro crystallites and vacancies and on the basis of significant structure theory. The theory also focuses on the radial distribution function of liquids. A two parameter model is presented for correlating the thermal conductivities of liquids. This method is extended to mixtures by using simple mixing rules. The calculated results of this theory show that the model can be used for the correlation of thermal conductivities of aqueous solutions and mixtures consisting of alcohols.

In recent years, the laser-induced transient grating (LITG) method has been extensively used for the detection of many kinds of relaxation phenomena (Yano, Fukuda and Hashi [13]).When applied for measurement of thermal conductivity; this method has several advantages over the conventional methods. A non contact measurement can be made on a small sample and in a short time. In this method two coherent laser pulse beams of the same frequency which intersect and interfere in an absorbing sample induce a spatially periodic temperature distribution (thermal grating) in the sample. This grating is probed by a laser and the temporal behavior of the Bragg diffracted beam intensity gives direct information about the decay of the grating due to heat diffusion. This technique has been used for water-ethanol solution.

A device for automatic thermal conductivity measurements have been developed (Julia, Renaud and Ferrand [6]). The principle for this device is a thin metallic wire, in thermal equilibrium with the liquid sample surrounding it, becomes a quasilinear heat source when it conducts an electric current. The corresponding Fourier equation leads to a relation between liquid thermal conductivity, temperature change of wire and the emitted heat quantity. A method is proposed for measuring the liquid thermal conductivity using thermistor probe (Lahoucine, Sakshita and Kumada [12]). A two dimensional model heat conduction model of a specimen including a thermistor probe is developed and calculated numerically. The thermal conductivity of the specimen is determined to minimize differences between the numerical and measured temperature histories. The liquids used for in this method are ethanol and gelatin aqueous solution.

ASTM D 2717(ASTM [1]) is the standard which is used for determination of thermal conductivities of liquids. The experimental setup consists of a straight four-lead, platinum

resistance thermometer element located centrally in a long, small diameter, borosilicate glass tube. The thermal conductivity is determined by measurement of the temperature gradient produced across the liquid sample by a known amount of energy introduced into the cell by electrically heating the platinum element. This thesis work is conducted by having the intent that it can be used to get a better understanding of the method to determine the thermal conductivity of transparent liquid so that the same study can be used to find the thermal properties of the molten salts. In last few years there are a couple methods developed (Williams and Clarno [9]) for determining the thermal conductivity of molten salts.

One of the studies (Ewing, Span and Miller [15]) has shown the actual apparatus to measure the thermal conductivity of molten salt FLINAK. The apparatus is called as a uni-axial apparatus for thermal conductivity measurement. The apparatus accommodated the liquid molten salt sample inside a centrally located Inconel bar. The radial heat loss through the inconel bar is minimized by surrounding it with thick guard rings. The thermal gradients within the bar and the compensating gradients inside the guard ring is established by direct current heaters at the top of each and by uniform air cooling at the base of each. Thirty thermal gradients are measured across the bar. FLINAK is tested using this method for thermal conductivity up to a temperature range of 900^0C.

A group of researchers (Martin and Lang [17]) calculated the thermal conductivity of water using a parallel plate method. They tested a film of water in a temperature range of 6^0C to 70^0C. The bottom plate is kept at constant low temperature with the use of a water circulation loop while the top plate is heated with electrical heater. Convection is neglected in this study by keeping the top plate hotter than the bottom plate. Also the

horizontal shape of the test section is one of the important factors in this study to keep the convection in a negligible regime. A study about the thermal conductivity of molten salts (Cornwell [10]) is conducted. This study also focuses on one of the important aspects which states that the mixtures of molten salts have a thermal conductivity which is less than the proportional mean of the constituent salts. (Kato, Kobayasi, Araki and Furukawa [8]) suggested the method for calculating the thermal diffusivity of molten salts by stepwise heating method. This method is based on electrical heating of a thin metal plate as a plane heat source in the molten salt. The plate thickness and the distance between the plate and the point of temperature measurement are the two crucial factors involved in this method. Water and Glycerin are used as the test liquids during this test. One of the studies (Castelli and Stanley [7]) proposed a method to calculate the thermal conductivity of water as a function of temperature and pressure. This method uses the improved form of concentric cylinder method for measurement of thermal conductivity of liquids. The losses due to heat are minimized in this technique. The tests are made for a sample of water at a pressure range of atmospheric to 1400 bars.

As water exhibits an exceptional behavior in that the thermal conductivity increases with temperature, rather than decreases, and in addition is not linear in temperature, there are several theories proposed (E. McLaughlin [4]) for the measurement of thermal conductivity of water. Most of the theories that are cited in the literature are broadly grouped on the basis of the form of the intermolecular potential. This thesis work is primarily carried out for water as the test fluid so along with the thermal conductivity, the absorption coefficient of water is also examined. As water is an absorbing medium the current research work is focused on conductive and absorbing medium. The convection

part of the heat transfer is eliminated by proper experimental arrangement which will be discussed in detail in the future sections. In view of the absorption coefficient of water a reasonable amount of research work has been accomplished in last few years in determining the methods and theories supporting it. (Terzic and Slivka [2]) proposed a method that focuses on the effect of the sample thickness on the measurement of absorption coefficient of water. This study uses photo acoustic spectroscopy technique to calculate the absorption coefficient of water. A Dual beam pulse laser experimental set up is used for measuring the distilled water absorption coefficient (Mercier, Gaillard and Lotrian [3]). A laser method (Ivanov, Kalinini, Kolesnik and Bondarenko [24]) is proposed in which a laser is flashed either from a ship or from a plane. The signal reflected by water changes its shape and time dependent parameter because of the scattering and the absorption process. The absorption coefficient is calculated as a function of time. An approximate analysis on water absorption coefficient is given (Coakley [11]) with the help of classical mechanics to describe the rotation of water molecule.

1.3 Motivation

The subject of thermal conductivity of liquids is important for two main reasons: firstly, because its study can help in giving a better understanding of the basic molecular processes involved in transport phenomenon in general and secondly, because of its significance in technological application. The need for the alternative source of fuel and the fact that the fossil fuels are continuously depleting are the main factors for the research and development task of this work. Hydrogen is identified as the fuel storage medium of the future. Hydrogen can be an excellent energy carrier medium if it can be

produced in an environmentally safe ways and the issues regarding the storage of hydrogen are solved. The New Generation Nuclear Power Plant concept is under research phase. Nuclear energy can be the primary and the abundant source of hydrogen production through the high temperature processes (1000^0C). The High Temperature Heat Exchanger (HTHX) is a part of the loop which connects the nuclear power plant to the thermo chemical loop where hydrogen production takes place.

One of the candidate materials for the HTHX is a molten salt named as FLiNaK. It is a eutectic alkaline metal fluoride salt mixture LiF-NaF-KF (46.5-11.5-42 mol %). It has become necessary to understand the thermal and physical properties of the candidate coolant, FLiNaK. This molten salt is a transparent liquid in its liquid state. The melting point of FLiNaK is 454 ^{0}C and the boiling point is 1570 ^{0}C . In order to understand the thermal behavior of the molten salt it is necessary to understand the processes through which the thermal properties can be evaluated. As the molten salt is transparent in nature in its liquid state it is related with water. The techniques used for determination of thermal conductivity of water can be verified for molten salt besides there are few issues like molten salt is highly corrosive in nature. The present work is aimed to propose a method for use in determining eventually the thermal conductivity of FLiNaK at high temperature. An attempt to validate this method will be accomplished here through testing with water and other transparent liquid like Glycerin and Glycol. To apply this method to higher temperature conditions for these molten salts necessary adaptation need to be made so that they can be suited for handling the liquid Flinak at 454 ^{0}C and also to take into account the corrosive nature of that material

1.4 Definition and Concept

Thermal conductivity is the intensive property of a material that increases its ability to conduct heat. It is defined as the quantity of heat Q, transmitted in time t through a thickness L, in a direction normal to surface area A, due to a temperature difference ΔT, under steady state conditions and when heat transfer is dependent only on temperature gradient.

The law that governs thermal conductivity is called as Fourier's Law and it can be stated as

$$k = -\frac{q''_x}{\frac{dT}{dx}}$$

Where

q''_x Is the heat flux and

$\frac{dT}{dx}$ Is the temperature gradient. The heat flux is in a direction normal to the area.

Thermal conductivity depends on various parameters of the material the most common are structure and temperature. Thermal conductivity is important in heat exchangers, nuclear power plant applications, building insulation materials and the various areas of thermal heat transfer. In general thermal conductivity of solid is larger than that of a liquid, which is larger than that of a gas. Since the intermolecular spacing is much larger and the motion of the molecules is more random for the fluid state than for the solid state, the thermal energy transport is less effective and therefore the thermal conductivity of gases and liquids is generally smaller than that of solids (Inropera and Dewitt, [22]). The thermal conductivity of any material increases with increase in heat flux.

1.5 Methods

In the last 20 years, a variety of experimental methods have been developed for the measurement of thermal conductivity in liquid. The methods may be divided into two categories

1. Non-Steady techniques
2. Steady-state techniques

The non-steady thermal conductivity measurement is one in which a time dependent perturbation in the form of a heat flux, is applied to a fluid initially in equilibrium. The thermal conductivity of the fluid is obtained from an appropriate working equation relating the observed response of the temperature of the fluid to the perturbation. The advantage of a non-steady technique is that the measurements can be made relatively quickly. The steady-state techniques include the measurement when the material that is being analyzed is in complete equilibrium. These techniques are based directly on integrated form of Fourier's Law. The steady state techniques gives out quick signals which is good for signal analysis but the disadvantage associated with these technique is that generally it takes a long time to reach required equilibrium.

1.5.1 Transient Hot-Wire Method

The ideal experimental set up for transient hot wire method is shown in fig1. The ideal instrument consists of an infinitely long (upto 100mm), vertical line source of radial heat flux, q, per unit length which is applied stepwise at time, $t = 0$ (Ho, [21]). The heat source which is supposed to lose heat only by conduction is immersed in an infinite fluid which is initially in an equilibrium state and which has temperature-independent physical properties. The line heat source is coincident with the axis of the cylinder coordinate

system. Thus the temperature rise of the fluid, ΔT above its equilibrium value, at the radial position, r, is given by the solution of the non-steady conduction equation

$\frac{\delta T}{\delta t} = \kappa * \nabla^2 T$ Along with the definition $\Delta T(r,t) = T(R,t) - T_0$

Where T_0 represents the equilibrium temperature of the fluid and κ (constant) its thermal diffusivity. $\kappa = \frac{\lambda}{\rho * c_p}$

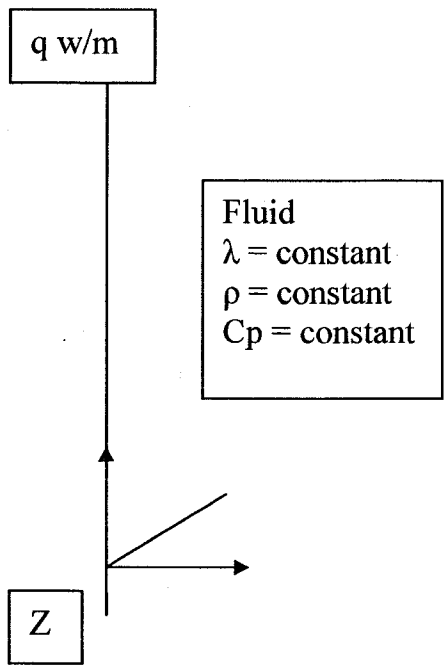

Figure1. The ideal model of the transient hot-wire method

1.5.2 Steady State Parallel Plate Method

The practical arrangement which most nearly approaches the one-dimensional heat flow characteristics of the infinite plates is shown schematically in fig 2(Ho, [21]). It consists of a flat, circular, horizontal upper plate, U, of radius, R_1, separated by a distance, d, from a larger, parallel plate, L, of radius, R_2. The plates are maintained at constant, uniform temperature, T_U and T_L, respectively ($T_U > T_L$). The upper plate is surrounded by a guard-plate, G, which is coplanar with U at its lower surface and is also maintained at the temperature, T_U. The guard plate is sufficiently close to the upper plate (b<<d) to eliminate the distortion of the temperature profile at the edges of its lower surface to all intents and purposes. The fluid is contained within the regions I and II of the cell. The fluid region I is bounded by an insulating film, F, which prevents the heat conduction through the fluid parallel to the plates. Thermal conductivity is calculated by using the equation

$$Q = \lambda * A * \frac{\Delta T}{d}$$

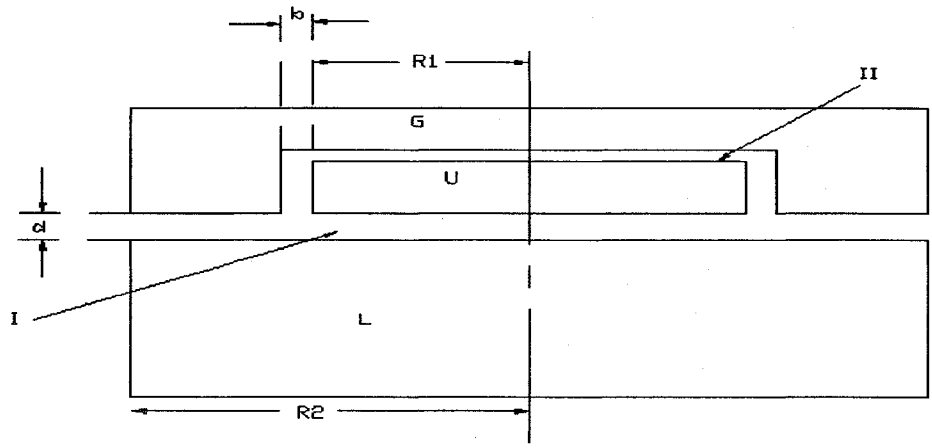

Figure 2. Model of a parallel-plate thermal conductivity instrument

1.5.3 The Concentric-Cylinder Method

The schematic of a steady state concentric cylinder thermal conductivity apparatus is shown in fig. 3. The inner cylinder with radius a and length l (upto 100mm) is supplied with heat at a rate Q to maintain it at steady uniform temperature, T_1. This inner cylinder is entirely surrounded by a close cylinder of internal radius b which is maintained at steady uniform temperature, T_2. The inner cylinder is separated from the internal surfaces of the ends of the outer cylinder by a layer of fluid which also fills the annular space. The loss of heat from the inner cylinder is assumed to be purely by conduction.

The thermal conductivity is calculated by following two equations

$$Q = \frac{2 * \Pi * l * \lambda}{\ln \frac{b}{a}} * \Delta T + G * \lambda = K * \lambda * \Delta T \quad \text{Where}$$

$$\Delta T = T_1 - T_2$$

λ is the thermal conductivity of the test fluid. G is a function of the dimensions of the cell. The function G describes the disturbance of the radial conduction process which occurs at the ends of the cell. G depends only on the length of the inner cylinder. The instrument constant K can be determined directly and very precisely by an independent measurement of the electrical capacitance of the cell.

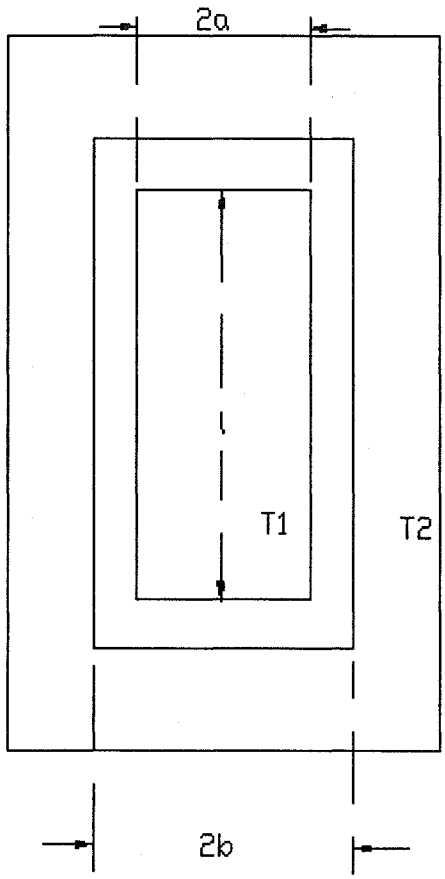

Figure 3. Model of a steady-state concentric cylinder thermal conductivity apparatus

CHAPTER 2

MATHEMATICAL MODEL

The purpose of this investigation is to provide an alternative insight into the heat transfer problem of a semi-transparent fluid with conduction heat transfer involved also. There exists little similarity between radiant heat transfer and the other modes of heat transfer that is conduction and convection. In a physical sense there are significant differences because radiation is transported by electromagnetic waves while conduction and convection involve contact between micro and macroscopic particles of matter. In a mathematical sense radiation problems must usually be formulated with integral equations. However, conduction and convection problems are usually formulated with differential equations. Conduction and radiation are governed by special cases of the integral equation which describes the most general transport processes. The effect of radiation in an absorbing medium (Viskanta and Grosh [19]) is illustrated extensively and the numerical approach is also provided.

When radiation is coupled with the other modes of heat transfer, the energy equation, which is normally a differential equation, becomes a nonlinear integro-differential equation. This comes about because the radiative contribution to the total energy flux is due, in part, to the geometrical configuration of the systems and reflections. There are no general solutions available for this integro-differential equation. In order to provide some insight into the problem of heat transfer by simultaneous conduction and radiation in an

absorbing medium, consideration is given to a one-dimensional system. The one-dimensional system consists of two diffuse, non-black, infinite, isothermal, parallel plates separated by a finite distance. The space between the plates is assumed to be filled with a thermal radiation absorbing and, of course, emitting medium.

2.1 Heat Transfer by Simultaneous Conduction and radiation

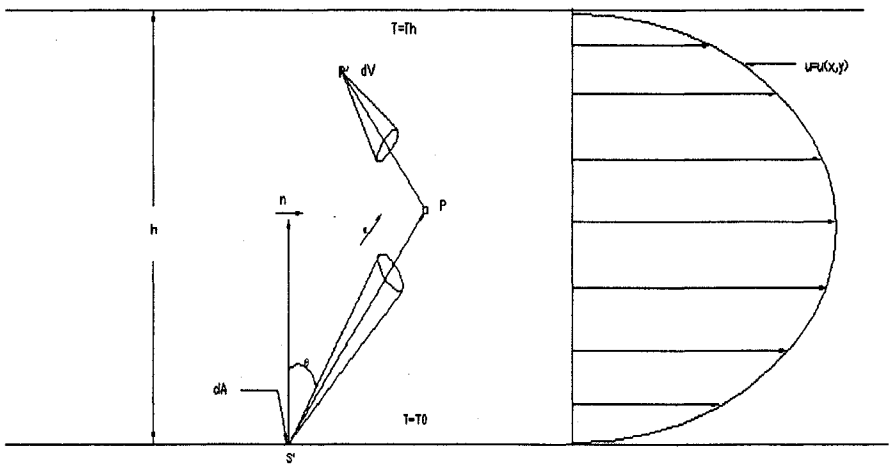

Figure 4. Physical Model and Coordinate System for Flow between Two Parallel Plates

The mathematical formulation for the heat transfer by simultaneous conduction and radiation is used here which is called as Rosseland's approximation. (Viskanta, [20]).

The following assumptions are used in the model

- The flow is steady and in the x-direction only.
- The physical properties are independent of temperature.

- The viscous dissipation of energy is negligible.
- There are no body forces and the energy generation due to pressure gradients is negligible.
- The surfaces are diffuse and radiosity on a surface is constant.
- The index of refraction of the medium is unity.
- The scattering is negligible compared to the absorption

The energy equation (Viskanta, [21]) is

$$\rho c_p u \frac{\partial T}{\partial x} = k\left(\frac{\partial^2 T}{\partial x^2} + \frac{\partial^2 T}{\partial y^2}\right) + q''' - \xi_n \qquad 1$$

Non dimensional zing the dependent and independent variables

$$\zeta = \frac{x}{l} \qquad \xi = \frac{y}{h} \qquad \theta = \frac{T}{T^*} \qquad 2$$

Where l and h are the longest dimensions in x and y directions, respectively, and T^* is an arbitrary temperature. The definitions of the dimensionless variables are arbitrary.

$$\text{Then } \frac{\partial T}{\partial x} = \frac{T^*}{l}\frac{\partial \theta}{\partial \zeta} \text{ and } \frac{\partial T}{\partial y} = \frac{T^*}{h}\frac{\partial \theta}{\partial \xi} \qquad 3$$

Substituting the new variables in equation 1

$$\frac{\rho c_p u T^*}{l}\frac{\partial \theta}{\partial \zeta} = \frac{kT^*}{l^2}\frac{\partial^2 \theta}{\partial \zeta^2} + \frac{kT^*}{h^2}\frac{\partial^2 \theta}{\partial \xi^2} + q''' - \varepsilon_n \qquad 4$$

Dividing both sides of equation 4 by $4\kappa\sigma T^{*4}$, which is the energy emitted by the unit volume of the medium at temperature T^* per unit time

$$\frac{\rho c_p u T^*}{4l\kappa\sigma T^{*4}}\frac{\partial\theta}{\partial\zeta}=\frac{kT^*}{4l^2\kappa\sigma T^{*4}}\frac{\partial^2\theta}{\partial\zeta^2}+\frac{kT^*}{4h^2\kappa\sigma T^{*4}}\frac{\partial^2\theta}{\partial\xi^2}+\frac{q'''}{4\kappa\sigma T^{*4}}-\frac{\varepsilon_n}{4\kappa\sigma T^{*4}} \qquad 5$$

This equation is a non –dimensional equation

$\frac{\rho c_p u T^*}{4l\kappa\sigma T^{*4}}$ = Energy content of the flowing fluid ÷ Energy radiated from the flowing fluid.

$\frac{kT^*}{4l^2\kappa\sigma T^{*4}}$ = Energy transfer by conduction in x direction ÷ Energy radiated in the x direction from the flowing fluid.

$\frac{kT^*}{4h^2\kappa\sigma T^{*4}}$ =Energy transfer by conduction in y direction ÷ Energy radiated in y direction from fluid.

$\frac{q'''}{4\kappa\sigma T^{*4}}$ =Energy generated in the fluid ÷ Energy radiated from the flowing fluid.

Consider the transfer of energy by conduction and radiation only. Also assuming that the energy transfer by conduction in the x direction is negligible compared with that in the y direction. Introducing the dimensionless temperature and dividing by $4\kappa\sigma T^{*4}$, the steady state energy equation 1 reduces to

$$\frac{kT^*}{4\kappa\sigma T^{*4}}\frac{d^2\theta}{dy^2}=\frac{\varepsilon_n}{4\kappa\sigma T^{*4}} \qquad 6$$

Since there is no temperature variation in the x direction, the distances can be measured in the units of the mean free path of radiation. Introducing the optical thickness, $\tau = \kappa y$ as the new independent variable. Utilizing the expression for net emission and putting it into energy equation 6, we get

$$\frac{k\kappa^2 T^*}{4\kappa\sigma T^{*4}}\frac{d^2\theta}{d\tau^2}=\frac{1}{2\sigma T^{*4}}\left[2E_{bb}(\tau)-E(0)E_2(\tau)-E(\tau_0)E_2(\tau_0-\tau)-\int_0^{\tau_0}E_1(|\tau-\tau'|)E_{bb}(\tau')d\tau'\right] \qquad 7$$

If the surfaces are assumed to be black, $E = E_{bb} = \sigma T^4$, equation 7 reduces to

$$N\frac{d^2\theta}{d\tau^2}=\theta^4-\frac{1}{2}\left[\theta^4(0)E_2(\tau)+\theta^4(\tau_0)E_2(\tau_0-\tau)+\int_0^{\tau_0}E_1(|\tau-\tau'|)\theta^4(\tau')d\tau'\right] \qquad 8$$

$$\text{Where} \quad N=\frac{k\kappa^2 T^*}{4\kappa\sigma T^{*5}}=\frac{k\kappa}{4\sigma T^{*3}}$$

The magnitude of this dimensionless parameter determines the relative role of the conduction term vs. the radiative terms. For large values of N conduction predominates, while radiation is the important energy transport process for small values on N. The importance of temperature in this parameter is obvious. The boundary conditions in dimensionless notation for equation 8 are

$$\tau = 0 (y = 0), \quad \theta(\tau) = \theta(0);$$

$$\tau = \tau_0 (y = h), \quad \theta(\tau) = \theta(\tau_0). \qquad 9$$

According to Rosseland's approximation (Viskanta, [20]) the radiant heat flux vector is given by

$$\vec{E}_\lambda = -\frac{1}{3\beta_\lambda} grad\varepsilon_\lambda \qquad 10$$

Substituting the diffusion approximation equation 10 into the energy equation for steady state, we obtain

$$div(-kgradT + \vec{E}) = 0 \qquad 11$$

For one dimensional case this equation reduces to

$$\frac{d}{dy}\left(k_{eff}\frac{dT}{dy}\right) = 0 \qquad 12$$

Where $$k_{eff} = k + k_r = k + \frac{16n^2\sigma T^3}{3\kappa} \qquad 13$$

Using the previously defined dimensionless independent variables $(\xi = y/h)$ and the boundary conditions

$$\frac{d}{dy}\left(k_{eff}\frac{dT}{dy}\right)$$

$$\frac{d}{dy}=\frac{1}{h}\frac{dT}{d\xi}$$

$$\int\frac{1}{h}\frac{d}{d\xi}\left[k+\frac{16n^2\sigma T^3}{3\kappa}\right].\int\frac{1}{h}\frac{dT}{d\xi}=0$$

$$\frac{k}{h}.\frac{dT}{d\xi}+\frac{16n^2\sigma T^3}{3k\kappa}.\frac{dT}{d\xi}=c_1$$

$$\frac{dT}{d\xi}\left(\frac{k}{h}+\frac{16n^2\sigma T^3}{3\kappa h}\right)=c_1$$

$$dT\left(\frac{k}{h}+\frac{16n^2\sigma T^3}{3\kappa h}\right)=c_1.d\xi$$

$$\int\frac{k}{h}dT+\int\frac{16n^2\sigma T^3}{3\kappa h}.dT=\int c_1 d\xi$$

$$\frac{k}{h}.T+\frac{4n^2\sigma T^4}{3h\kappa}=c_1\xi+c_2$$

Using the boundary conditions

$$\xi=0 \qquad T=T_0$$

$$\xi=1 \qquad T=T_h$$

At $\xi = 0$,

$$\frac{k}{h}.T_0 + \frac{4n^2\sigma T_0^{\,4}}{3h\kappa} = c_2$$

$$\frac{k}{h}.T + \frac{4n^2\sigma T^4}{3h\kappa} = c_1\xi + \frac{k}{h}.T_0 + \frac{4n^2\sigma T_0^{\,4}}{3h\kappa} \qquad 14$$

At $\xi = 1$

$$\frac{k}{h}.T_h + \frac{4n^2\sigma T_h^{\,4}}{3h\kappa} = c_1 + \frac{k}{h}.T_0 + \frac{4n^2\sigma T_0^{\,4}}{3h\kappa}$$

$$\frac{k}{h}.(T_h - T_0) + \frac{4n^2\sigma}{3h\kappa}.\left(T_h^{\,4} - T_0^{\,4}\right) = c_1$$

$$\frac{k}{h}.T + \frac{4n^2\sigma T^4}{3h\kappa} = \left[\frac{k}{h}.(T_h - T_0) + \frac{4n^2\sigma}{3h\kappa}.\left(T_h^{\,4} - T_0^{\,4}\right)\right]\xi + \frac{k}{h}.T_0 + \frac{4n^2\sigma T_0^{\,4}}{3h\kappa}$$

Multiplying both sides of the above equation by $\frac{h}{k}$

$$T + \frac{4n^2\sigma T^4}{3k\kappa} = T_h.\xi - T_0.\xi + T_0 + \frac{4n^2\sigma T_h^{\,4}}{3k\kappa}.\xi - \frac{4n^2\sigma T_0^{\,4}}{3k\kappa}.\xi + \frac{4n^2\sigma T_0^{\,4}}{3k\kappa}$$

$$T + \frac{4n^2\sigma T^4}{3k\kappa} = \left[T_0.(1-\xi) + T.\xi\right] + \frac{4n^2\sigma}{3k\kappa}.\left[T_0^{\,4}.(1-\xi) + T_h.\xi\right] \qquad 15$$

The equation 15 is the non linear equation. This equation is used in conjunction with the experimental temperature values to find the optimized values for thermal conductivity (k) and absorption coefficient (κ).

CHAPTER 3

EXPERIMENTAL SET-UP

3.1 Validity of Test Fluids

The experimental set up is based on (Yoshida, Fujisaki and Washio [14]) the previous study carried out for the simultaneous measurement of the thermal conductivity and absorption coefficient of radiation by arbitrary heating. This method is proposed for semi-transparent liquid and it is a transient state method. Water is used as the primary test fluid in the ongoing research work. It has become necessary to verify the competency of the candidate test fluid so as to check if it can absorb radiation for a reasonable amount of depth or not. Research work has been conducted to verify the attenuation property of water (Hale and Querry [25]). Similarly from the study of heat transfer in liquid bath (Komarov and Sano [31]) and the handbook of optical properties of materials (Rolf [32]) it is clear that Glycerin and Ethylene Glycol also posses a reasonable amount of penetration depth. The result of (Hale and Querry) is shown in the following diagram.

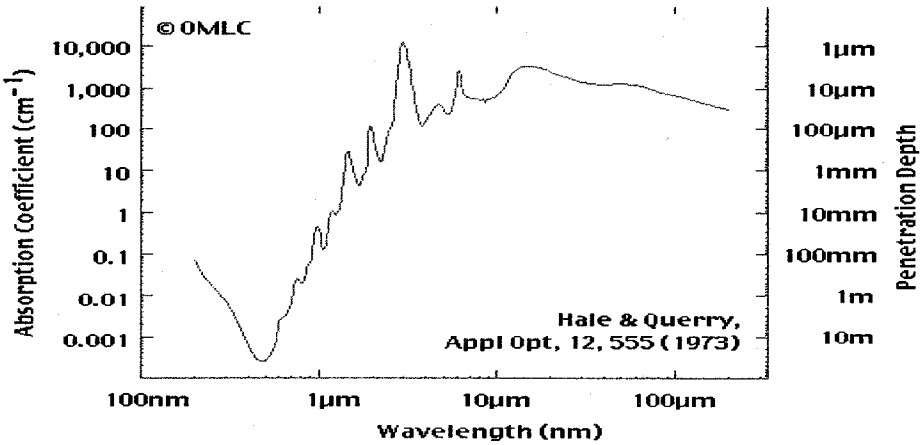

Figure 5. Absorption Spectrum of water

Similarly, (Seglestein, [26]) has shown that water can absorb radiation in the visible region up-to a good amount of depth.

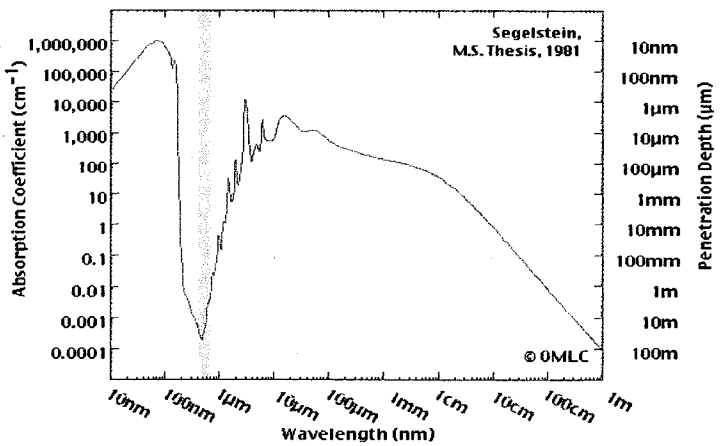

Figure 6. Complex refractive index of water.

3.2 Experimental Set-Up

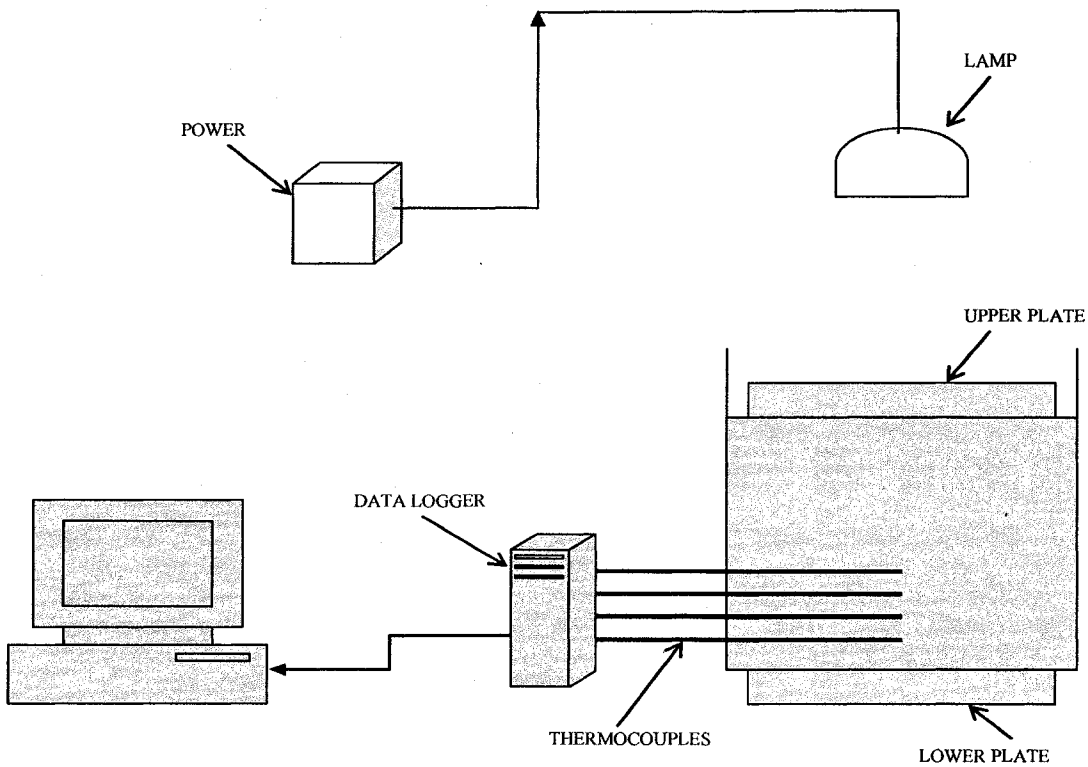

Figure 7. Schematic model of the experimental set-up

3.3 Hardware

The list of the hardware that is used in the experiment set up is listed below.

1. DC Power Supply
2. Thermoelectric Cold Plates
3. Temperature Controller
4. Data Acquisition
5. Halogen Light Bulbs
6. Ceramic Tubes
7. K-Type Thermocouple
8. Thermocouple Connectors
9. PVC-Pipe
10. Aluminum Plates
11. Silicon RTV
12. Ceramic Fiber Strip Insulation
13. Metallic Tape

The three types of test fluids that are used are given below

1. Water
2. Glycerin
3. Ethylene Glycol

Few of the above mentioned hardware parts are discussed in detail in the following tables.

1. D.C. Power Supply

The following table shows the details of the D.C. Power supply that has been used to carry out the experiments

Working temperature	-10^0C to 60^0C
Output Voltage	+12VDC@0-12.5A
Power Density	2.24W/in3
Universal AC Input	88-132/176-264VAC@47-63Hz
Inrush Current	@120VAC:35
Isolation Voltage	3000
Leakage Current	3.5mA@240V
Efficiency	82%
Weight	1.8lbs.
Dimensions	7.8X4.3X2.0Inches

Table 1. Properties of the D.C. Power Supply

Source: Advanced Thermoelectric Inc.

Figure 8. D.C. Power Supply

2. Thermoelectric Cold Plates

The TCP-100 Cold Plates are used in the experiment as the cooling source. This cold plate posses a cooling capacity of 100Watts.

Operating Temperature	-15^{0}C to 75^{0}C
Cooling Capacity	100W at 25^{0}C ambient temperature
Heating Capacity	100W w/25^{0}C ambient air
Nominal Voltage	12VDC(Max=15VDC)
Current	8.5 Amps@12VDC
Cooling Fan	Brushless, Nominal 12 VDC
Fan Life	50,000 hours
Dimensions	4X8X3 5/8 Inches
Weight	4lbs.

Table 2. Properties of the Thermoelectric Cold Plates

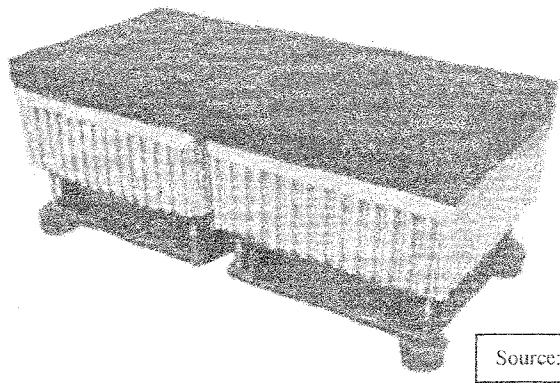

Source: Advanced Thermoelectric Inc.

Figure 9. Thermoelectric Cold Plates

3. Temperature Controller

TLZ-10 is used as the temperature controller to control the temperature of the cold plates.

Input Power Required	12VAC/VDC (50/60Hz)
Power Consumption	3VA
Control	On/Off
Input	Programmable Input for PTC-KTY 81-121
Sampling rate	1 per second

Table. 3. Properties of Temperature Controller

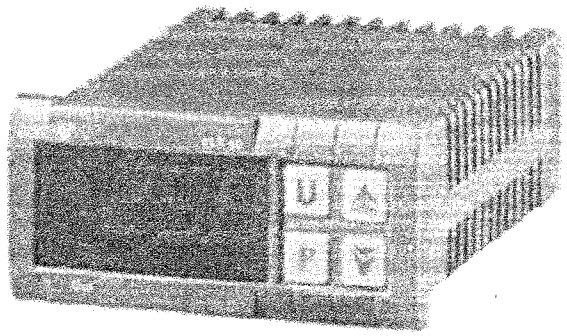

Figure 10. Temperature Controller

Source: Advanced Thermoelectric Inc.

4. Data Acquisition

This particular DAQ system is used in conjunction with PCI 4351 card.

The DAQ system has following peculiarities.

- 68-pin DIN-rail mountable terminal block with screw terminals.
- 14 Unconditioned temperature and voltage inputs.
- Built in Cold-Junction compensation and Auto Zeroing Circuitry.
- It has isothermal design , plastic cover to minimize the thermal gradients across the terminal block

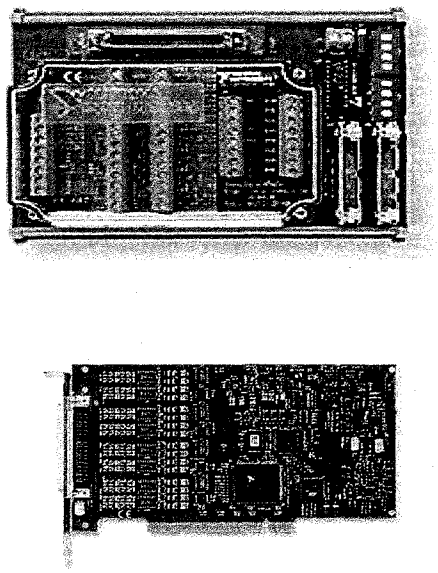

Figure 11.DAQ and PCI 4351

Source: National Instruments Inc.

5. Halogen Bulb

Two different Halogen Bulbs of 40 W and 60W are used as the source of the heat flux for the experiments.

6. Ceramic Tubes

The Ceramic Tubes are used in the set up as the guard tubes through which the thermocouple wire is passed. The characteristics of the Ceramic Tubes are listed below.

Constitution	80% Mullite and 20% Glass
Water Absorption	0.00
Specific Gravity	2.4
Gas Permeability	Gas Tight
Maximum Service Temperature	1600^{0}C

Table. 4. Properties of Ceramic Tube

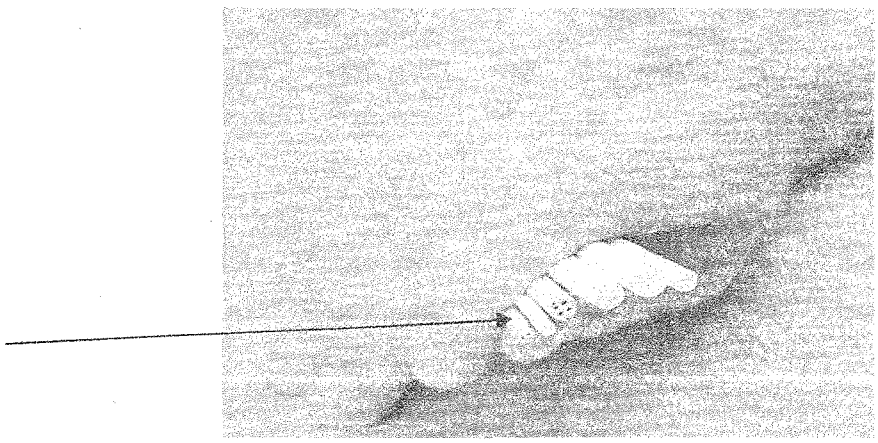

Figure 12.Ceramic Tube

Source: Omega Inc.

The thought process for using two different kinds of halogen bulbs is to show the robustness of the experimental and associated with it the numerical method. Also the use of cold plates is made on the same ground. The cold plate is kept at three different temperatures and these three temperatures provided three different lower boundary conditions. By using the cold plates and the halogen bulbs an attempt is made to show the parametric capabilities of the work. The following chapter reveals that the values of thermal conductivity and the absorption coefficient are almost constant for each fluid. The reason to for this is that the temperature range is not changing rapidly between different combinations of the heat source and the lower boundary condition imposed by the cold plates.

3.4 Description of the Experimental Set Up

The experimental set up designed in such a way that the conduction with radiation effect on the test fluid is taken into consideration. Broadly the crux of the work is to get the temperature profile of the test fluid at different steady boundary conditions and different heat sources. In this particular work the effect of convection heat transfer is neglected by setting up the apparatus in such a manner that it the top portion of the test section is heated with the heat source and the bottom portion is kept cool at constant temperature with the help of the thermoelectric cold plates and the temperature controller associated with it. Heat loss from the test section is the most important factor taken into consideration in the design of the equipment. This particular aspect of the work backs up the choice of using PVC as the material for the test section than any other metal. As PVC has the low thermal conductivity (0.20 W/m.K) (Incropera and Dewitt [22]), the heat loss through the sides of the test section can be eliminated. The test section is limited to a

height of 50mm. As water attenuates radiation (Hale and Querry [25]) up to a reasonable amount of depth (1m). Also the design calculation with only conduction considered and no radiation has shown that 50mm is reasonable channel height which can give up to a maximum temperature difference of 40^0C-50^0C. Of course it is expected that with radiation present that temperature difference will be somewhat less for the same amount of heat transmitted axially. This temperature range of the given test fluid (Water, Glycerin and Ethylene Glycol) is also manageable at the laboratory level which does not need any particular type of precautions or equipments as a safety measure and will certainly not create the conditions for boiling of any of these three fluids. The thickness of the test section is 3mm. K-type of thermocouples are used to monitor the temperature. The diameter of the thermocouple wire is 0.08mm. The type of thermocouple that has been used in the work has a maximum temperature range of 260^0C. This particular type of thermocouple has accuracy in the range of $\pm 1^0$C. In order to get the accurate temperature profile of the test fluid the thermocouples are run up-to the centre of the test section.

The diameter of the test section is 100mm. As the thermocouple wires with the PFA coating on them are very flexible and can not stand of their own to run up-to the centre of the test section, ceramic tubes with two holes are used. The ceramic tubes have two holes and each wire of the thermocouple (positive and negative) runs through each hole and the probe is situated accurately at the centre of the test section which is 50mm from the inside edge of the test cylinder. The selection of ceramic tubes instead of any other materials is based on some of the properties of the ceramic tubes. Basically the ceramic tubes are made of Mullite (80%) and Glass (20%), both of these materials have thermal

conductivity. So there does not remain any ambiguity that the heat supplied to the test section is absorbed by any other material than the test fluid. Also water absorption for ceramic is 0.00 which itself explains that it is water reluctant. This particular property of the ceramic tubes becomes one of the vital reasons for selection. Aluminum plates are used as the top and bottom plates for the test section. Because of the high thermal conductivity of aluminum (280W/m.K), it acts as the best carrier of heat from the heat source to the test fluid. The thickness of the aluminum is taken as 1mm. The reason for choosing the least thickness of the aluminum plates is that the to curb on the resistance offered by the increased thickness. More the thickness of the plates more is the resistance offered to the flow of heat and which reduces the amount of heat supplied to the test fluid.

The test section is insulated using the ceramic fiber strips. The ceramic fiber strips have a very low thermal conductivity. Also the strips are easy to use and can be formed into complex shapes. The thickness of the ceramic strip is 1/8inch. To provide additional support and to maintain the insulation on the test section intact a metal tape is used to wound around the complete assembly. The position of the thermocouples is an important factor while designing the experimental set up. As the problem at hand needs attention given to conduction and radiation it has become vital to choose the placement of the thermocouples. There are 8 thermocouples that are used to get the temperature profile. In order to get the exact temperature profile at the centre of the test section all 8 thermocouples are placed across the periphery of the circular test section as shown in following diagrams and pictures. The distance between the probes of one thermocouple to the other is 6mm. The lowest thermocouple from the bottom side of the test section is

placed at a distance of 1mm from the bottom edge of the test section. And the top most thermocouple is also placed at 1mm from the top most edge. The thermocouples are connected to the DAQ box with the help of the thermocouple connectors. The advantage of using the connectors is that the thermocouples are given long length of wire which ultimately gives leverage to place the DAQ box and also to work around such a closely packed assembly.

The halogen bulbs of 40W and 60W are used as the source of heat flux for the experiment. The bulbs are hung from the bar which has a socket of 1 1/16" size. Both the bulbs have the base diameter of 1 1/16". A PVC pipe is used to flow the power wire supplied to the halogen bulbs as shown in the following diagrams. The PVC pipe has three different levels of arrangements which help in lowering and pushing up the bulbs. This particular arrangement is created so as to give some open space for the distance between the heat source and the top most plate of the cylinder. The normal distance between the halogen bulb and the test section is 2inches. The complete assembly is set on a wooden structure which is in L shape with two plywood sheets of 18inchesX18inches. The thickness of the plywood sheets is 3/4". The DC power supply and the temperature controller is mounted on the vertical plywood sheet. This helps in reducing the risk of any possible short circuit which can happen with any leakage from the test section if the DC power supply and the test section are mounted on the same platform. Silicon RTV is used as the gasket sealant and adhesive for all the joints that are created in the experimental set up. The operating temperature range of RTV is up to 400^0C. This particular property of the RTV is very helpful which insures that there might not be any possible leakages because of the increased temperature in the test section. Also RTV acts as neutral with all

the three test liquids that are taken into use. RTV gains its full strength after application within 24 hours span. The assembly of the experimental parts and the final set up is shown in the following figures.

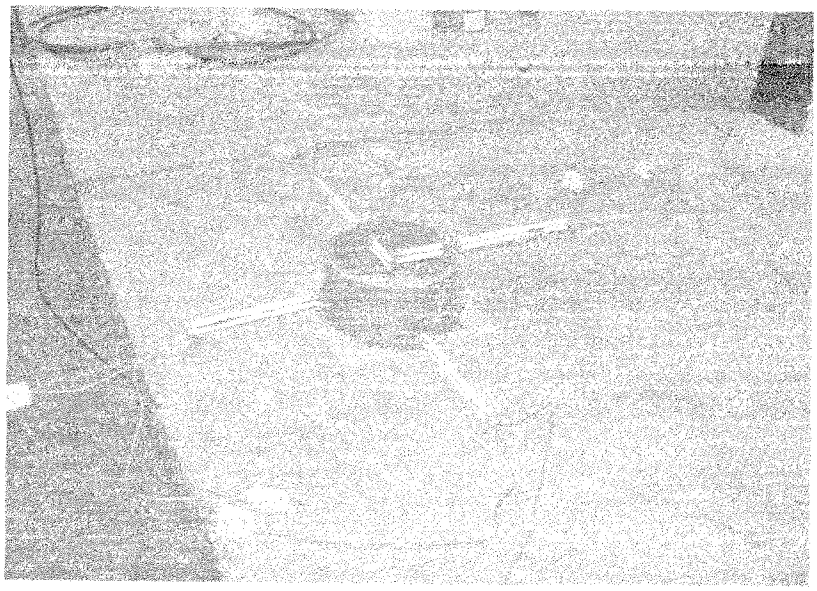

Figure 13. Test section with thermocouples and connectors

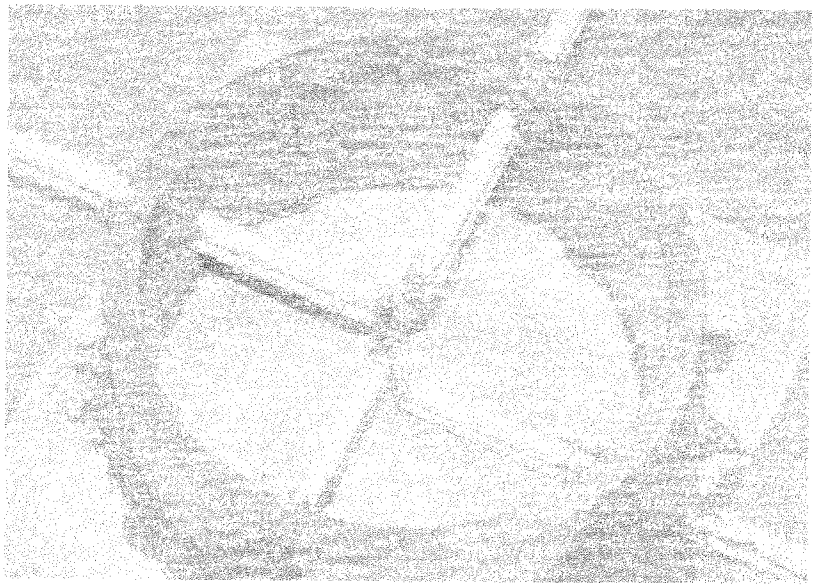

Figure 14. Thermocouples are run to the centre with probe at centre

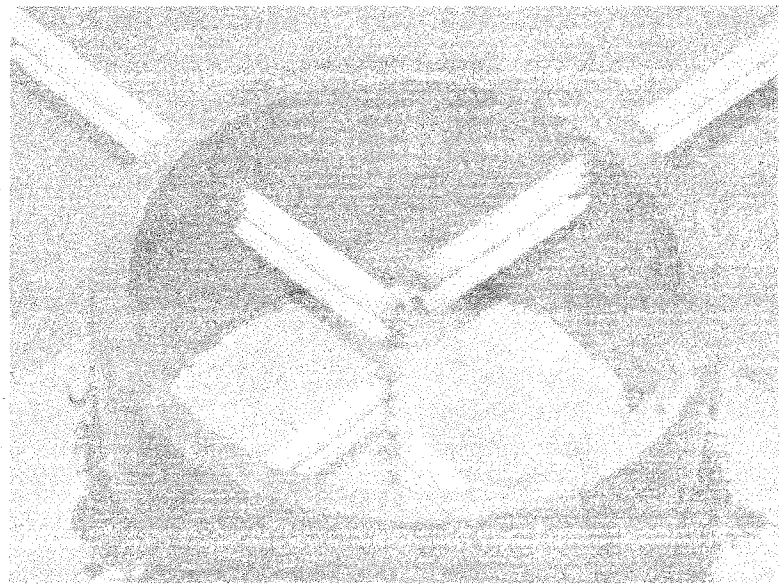

Figure 15. Thermocouple probes are placed 6mm from one above the other

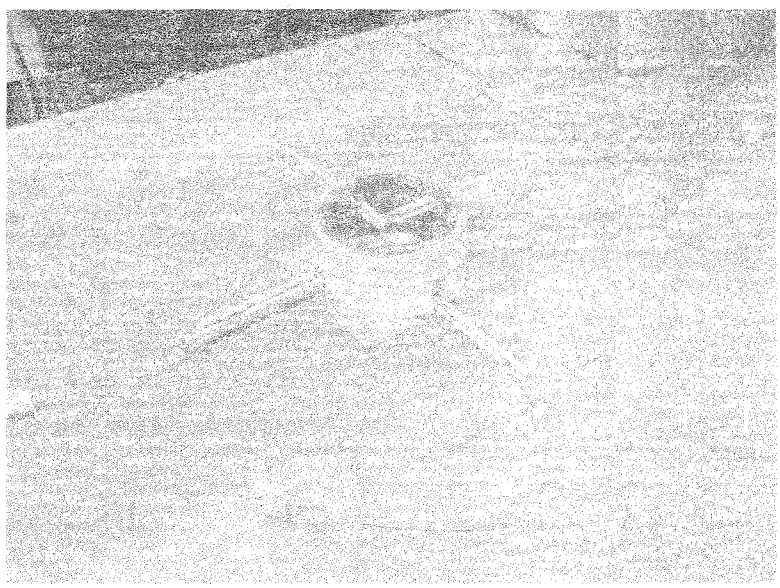

Figure 16. Ceramic fiber strip is used as insulating material

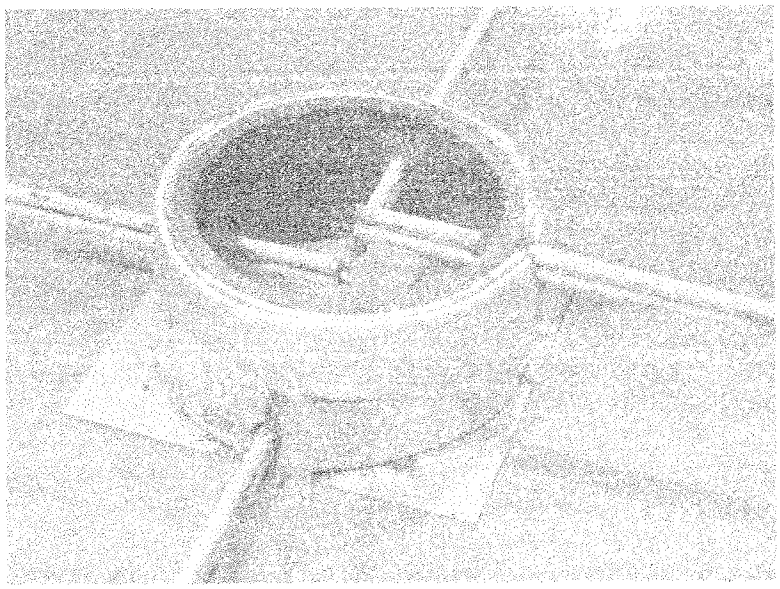

Figure 17. Aluminum tape is used to provide strength to the insulation

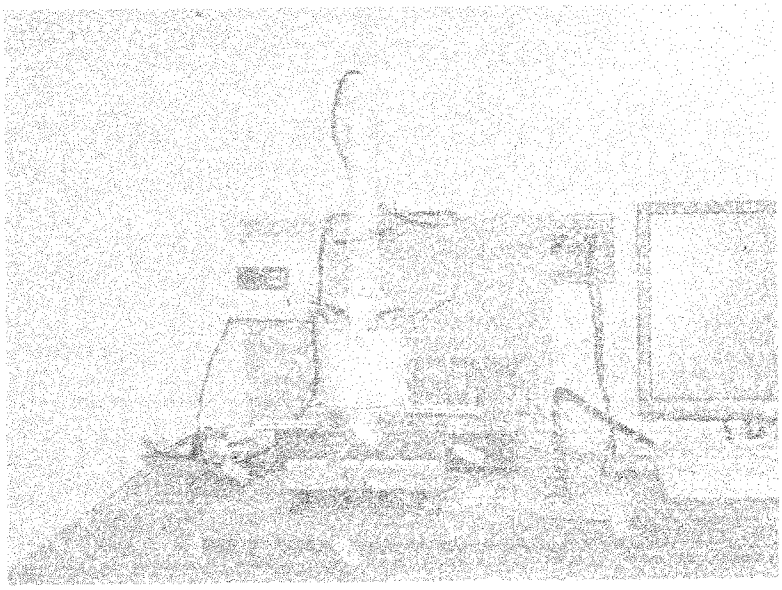

Figure 18. The final set-up

CHAPTER 4

RESULTS

The experiments are carried out using three different types of test fluid as

- Water
- Glycerin
- Ethylene Glycol.

In order to get a better degree of understanding three different steady state boundary conditions are employed during the course of experiments. The bottom boundary of the test section is maintained at following three different temperatures for each of the test fluid

- 5^0C
- 10^0C
- 15^0C

The heat source that is used in solving the conduction and radiation problem is a halogen bulb. Two different wattages of halogen bulbs are used to provide the heat which is used to heat the top plate of the test section. The two wattages of the halogen bulbs that are used are

- 40W
- 60W

Thus for each test fluid there are 6 tests conducted. The diffusion equation (equation 15) is solved in Mat lab. It is a equation with two parameters to be optimized. The diffusion equation is an output of the Roseland's Approximation which is used as the basis of this work. As it is an equation with two variables and two unknown there are infinite solutions for each set of experimental results. The temperature distribution that has been obtained form the experiments is supplied to the Mat Lab code in order to find the thermal conductivity and the absorption coefficient of the test liquid. The thermal conductivity and the absorption coefficient are the two unknown of the diffusion equation.

As the diffusion equation is a non linear equation the optimization tool box of the software Mat Lab is used. The diffusion equation 15 is taken on one side of the equation in Mat lab and the other side of equation is made zero. The function fzero is used in Mat Lab. The values of dimensionless variable zeta are given in the code. The zeta is the height at which the eight thermocouple are placed. The eight values of the temperature that are obtained from the experiments are fed to the program. These values of the temperatures match with the zeta values. The diffusion equation is solved in such a way that one side of the equation should go to zero. But as it is a non linear equation, a tolerance of 1e-6 is set for solving the problem. The fzero function of Mat lab searches for those values of k and κ which will try to meet the tolerance limit set for solving the equation. Guess values are supplied in order to solve the equation. The fzero function solves the equation and gives out the optimized values. The error function is defined as the square value of the difference of the experimental temperature and the temperature obtained by the code. The function fzero is a function of temperature. It is solved in such

a manner so as to incorporate the fact that conductivity is the function of temperature and the aim is to find the change in conductivity with different values of temperature obtained for each test fluid, for different settings of the heat source and the cold plate boundary condition.

The following diagrams show the result for water. The temperature distribution for 3 different boundary conditions and two different heat sources are shown here. Total there are 6 readings for each test fluid. There are eight thermocouples place din the test section.

I. water

A. 60W

A.1 5^0C Boundary condition

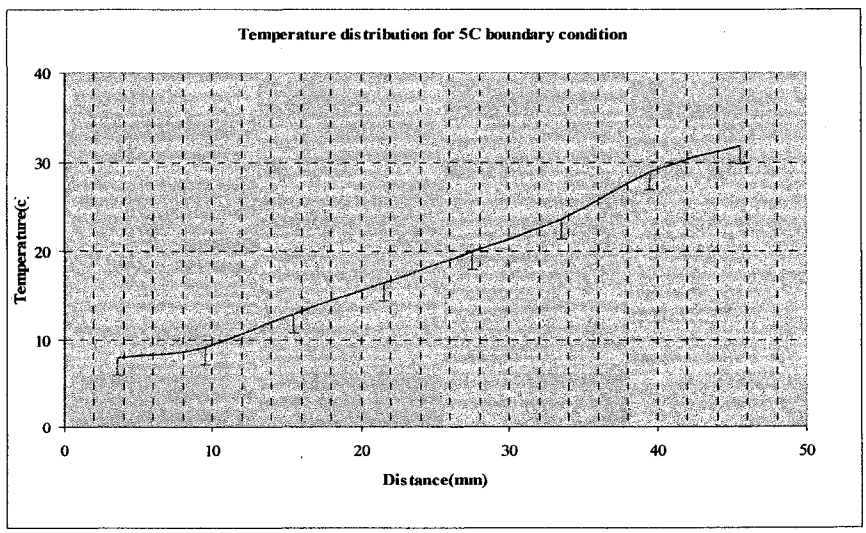

Figure 19. Temperature distribution for water with 5^0C boundary condition

A.2. 10^0C Boundary Condition

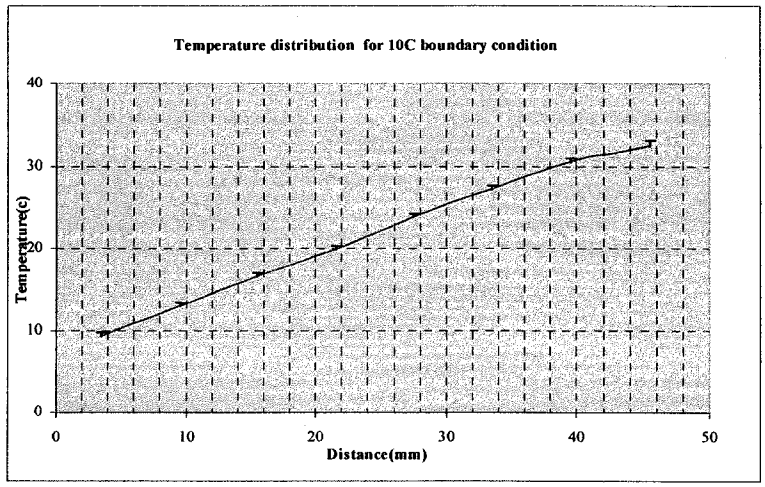

Figure 20. Temperature distribution for water with 10^0C boundary condition

A.3. 15^0C Boundary Condition

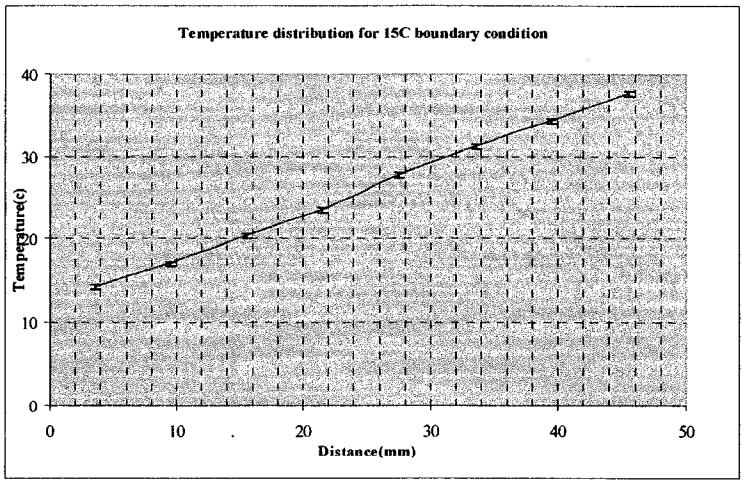

Figure 21. Temperature distribution for water with 15^0C boundary condition

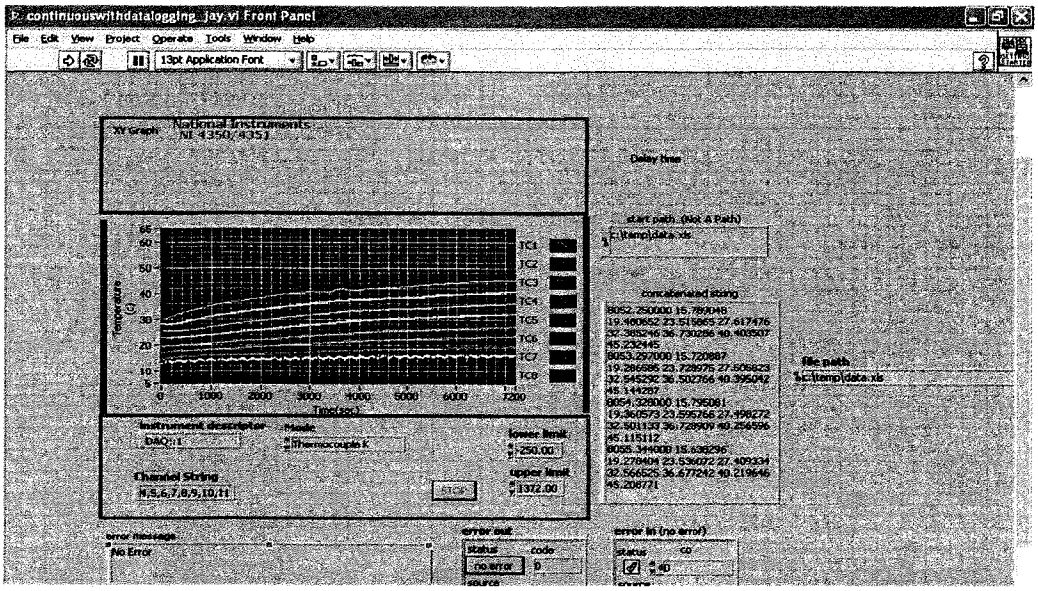

Figure 22. Diagram showing steady state for water

B. 40W

B.1. 5^0C Boundary condition

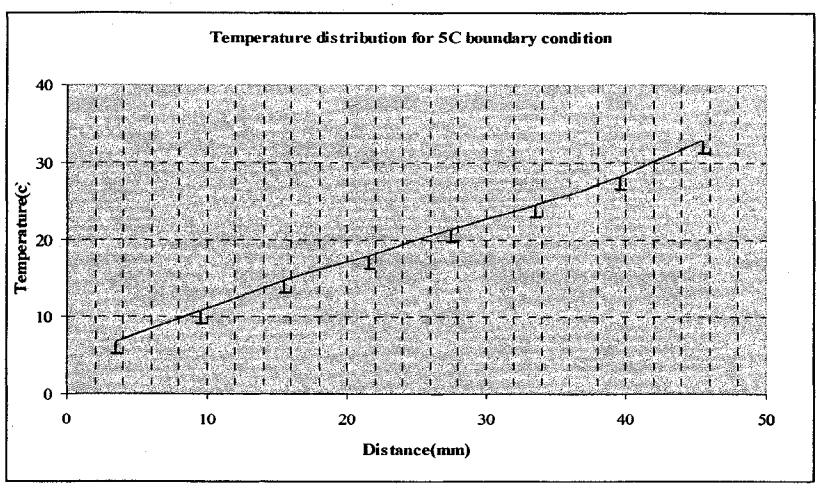

Figure 23.Temperature distribution for water with 5^0C boundary condition

B.2. 10^0C Boundary condition.

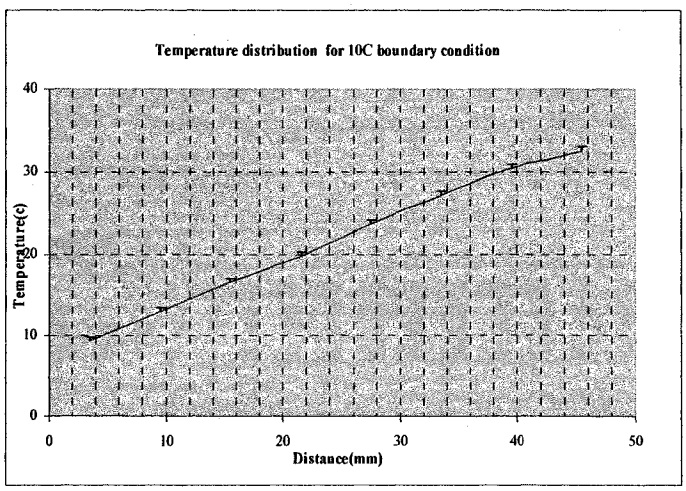

Figure 24.Temperature distribution for water with 10^0C boundary condition

B.3. 15^0C Boundary Condition

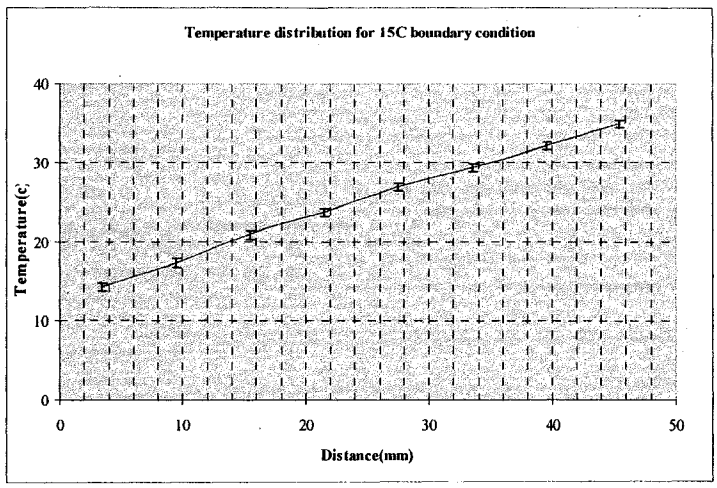

Figure 25. Temperature distribution for water with 15^0C boundary condition

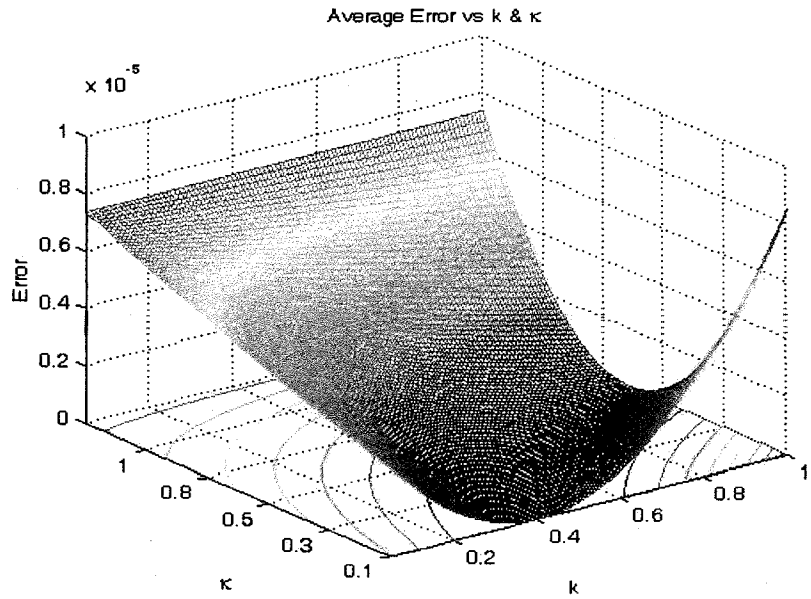

Figure 26. Plot showing the thermal conductivity and absorption coefficient of water

The above figure shows the result of the optimization technique that has been used to optimize the two parameters k and κ. The error function is defined so that it finds the optimized values of these two parameters which give the minimum error between the experimental temperature and the temperature profile that is calculated by the code. There are 48 temperature nodes used in solving the optimization problem. Each test fluid has 6 readings and each reading includes the temperature profile of 8 thermocouples.

The error function is written as

$[(T_{exp}-T_{calc})/T_{exp}]^2$.

The minimum value of the function gives the values of thermal conductivity.

For water the values of k and κ are as follows

k=0.64W/m.K

$\kappa=0.5cm^{-1}$

II. Glycerin

A.1. 5^0C Boundary condition

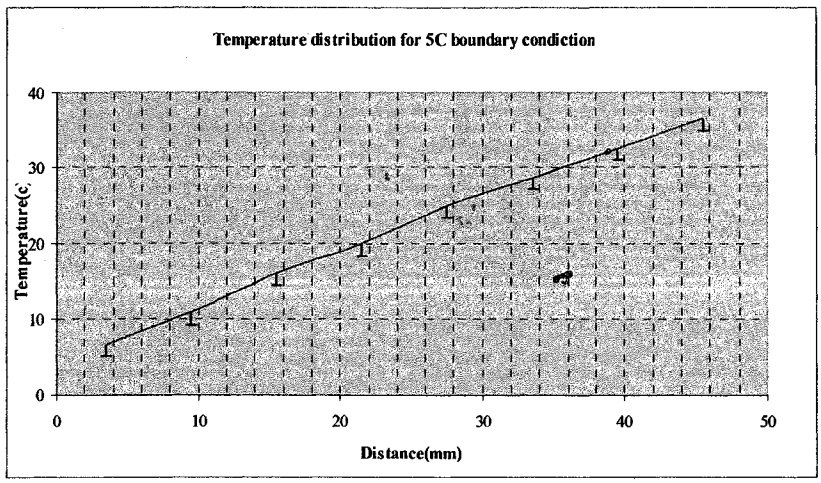

Figure 27. Temperature distribution for glycerin with 5^0C boundary condition

A.2 10^0C Boundary condition

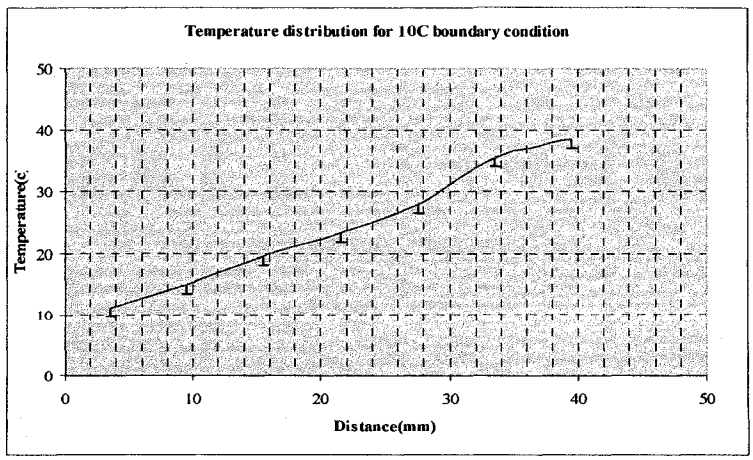

Figure 28. Temperature distribution for glycerin with 10^0C boundary condition

A.3. 15^0C Boundary condition

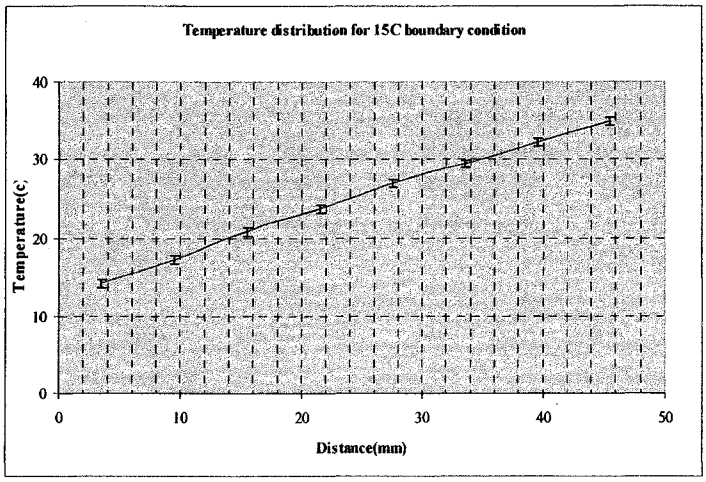

Figure 29. Temperature distribution for glycerin at 15^0C boundary condition

B. 40W

B.1. 5^0C Boundary condition.

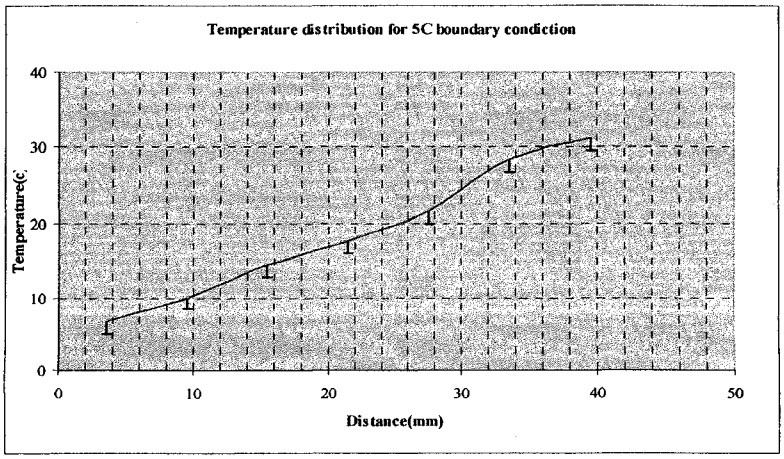

Figure 30. Temperature distribution for glycerin at 5^0C

B.2. 10^0C Boundary condition.

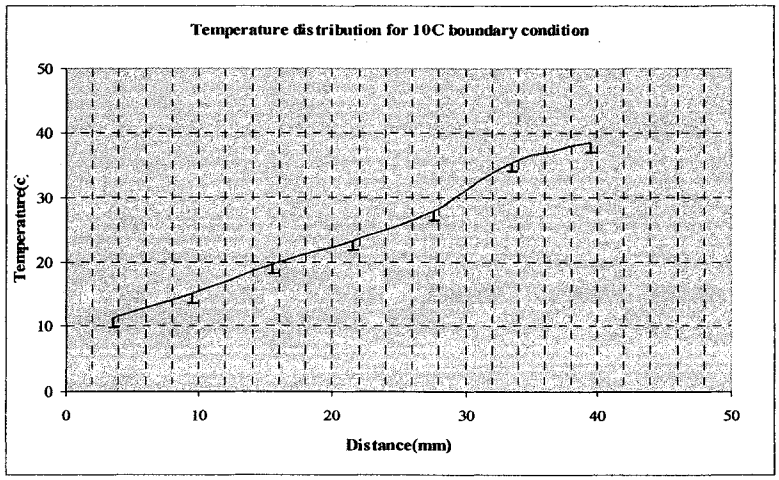

Figure 31. Temperature distribution for glycerin at 10^0C boundary condition

B.3. 15^0C Boundary condition

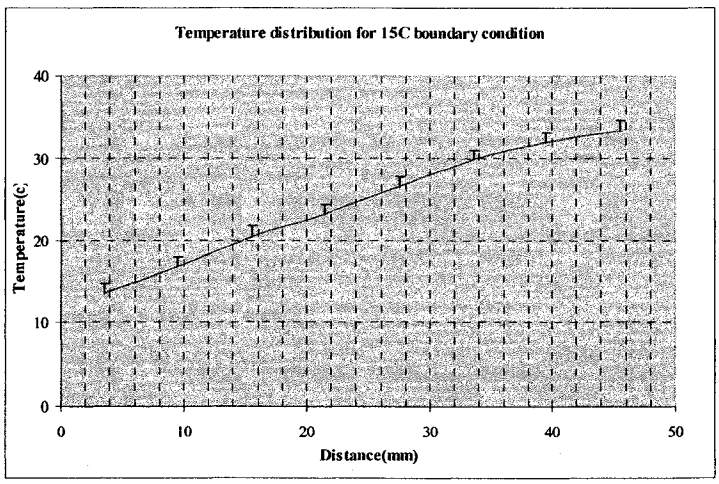

Figure 32. Temperature distribution for glycerin at 15^0C boundary condition

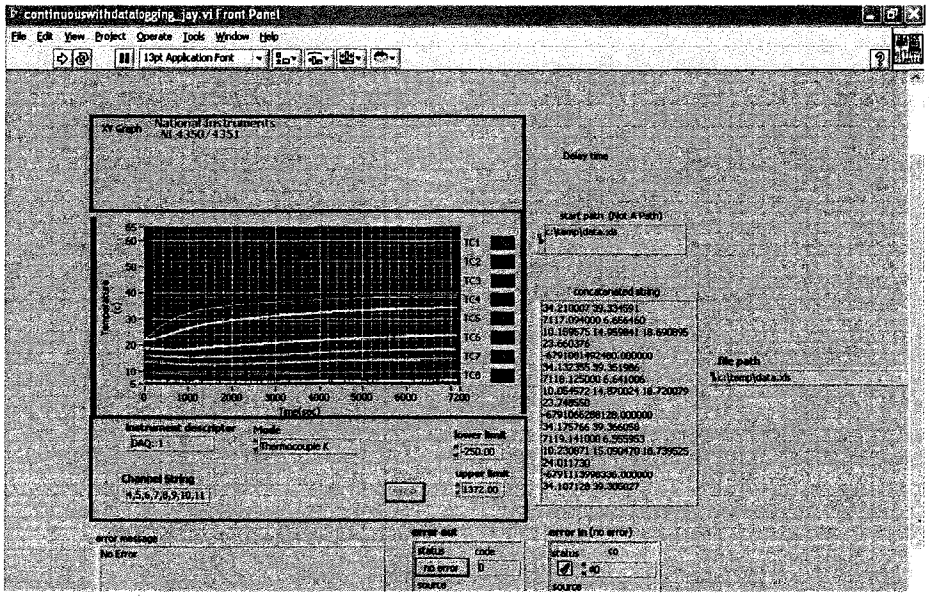

Figure 33. Diagram showing steady state for Glycerin

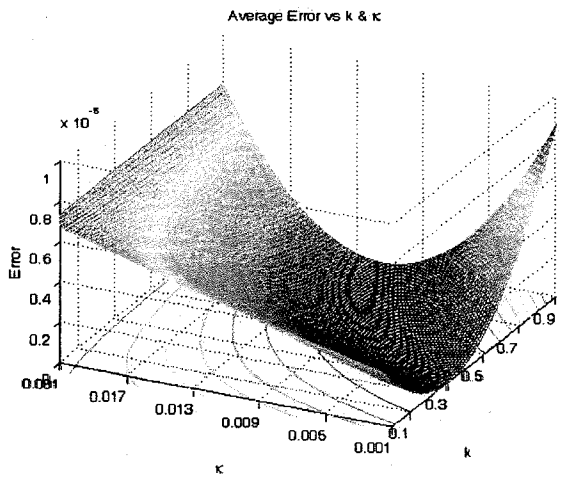

Figure 34. Graph for conductivity and absorption coefficient of Glycerin

k=0.32 W/m.K

$\kappa=0.002cm^{-1}$

III. Ethylene Glycol.

A.1. 5^0C Boundary condition.

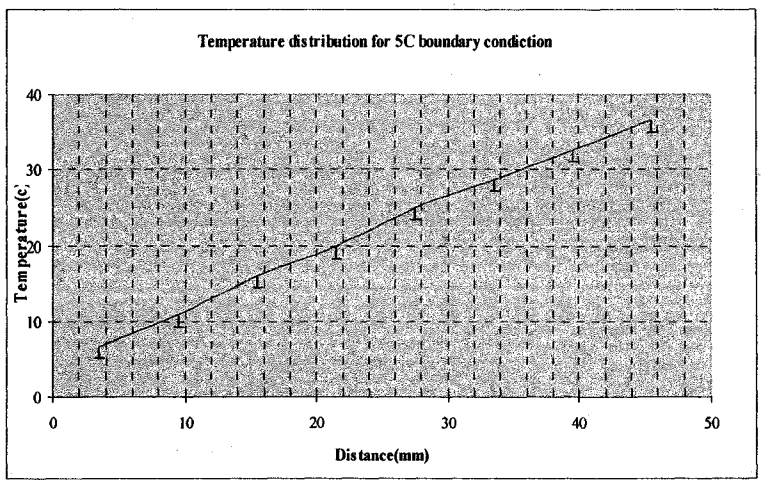

Figure 35. Temperature distribution for glycol at 5^0C boundary condition

A.2. 10^0C Boundary condition

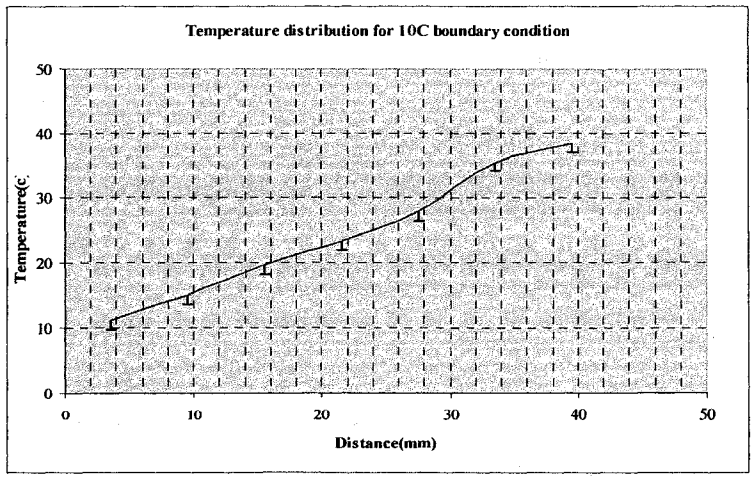

Figure 36. Temperature distribution for glycol with 10^0C boundary condition

A.3. 15^0C Boundary condition

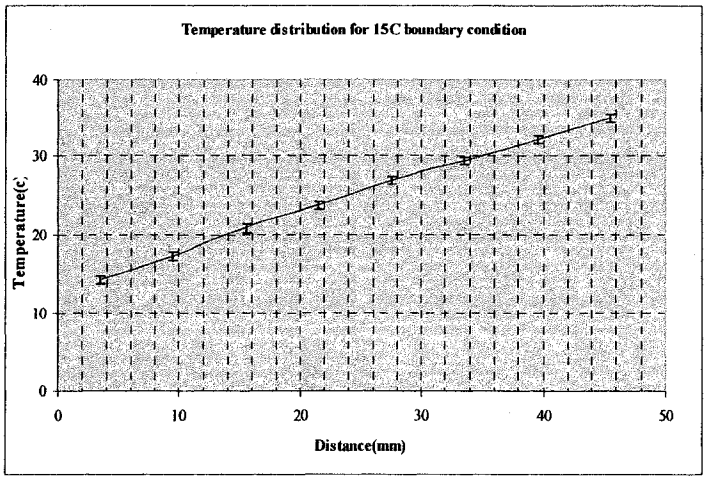

Figure 37. Temperature distribution for glycol at 15^0C boundary condition

B.1. 5^0C Boundary condition

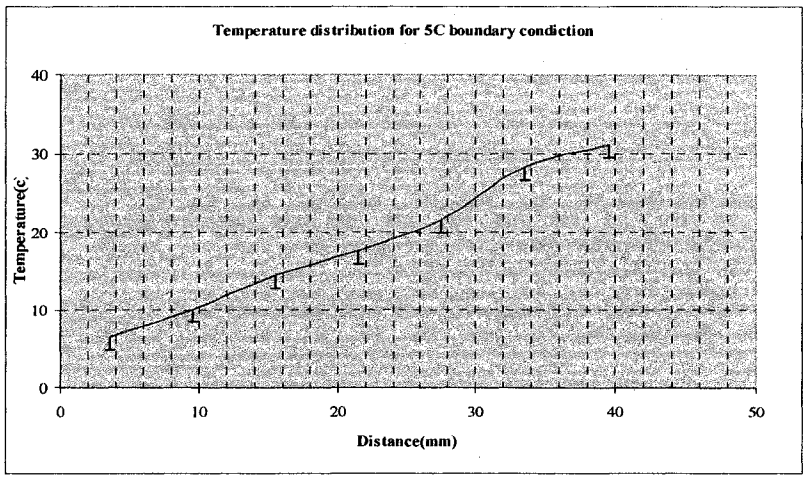

Figure 38. Temperature distribution for glycol at 5^0C boundary condition

B.2. 10^0C Boundary condition

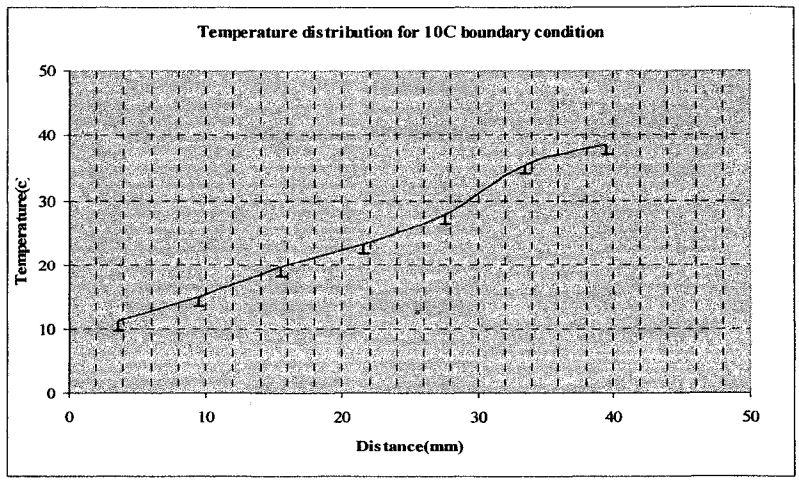

Figure 39. Temperature distribution for glycol with 10^0C boundary condition

B.3. 15^0C Boundary condition

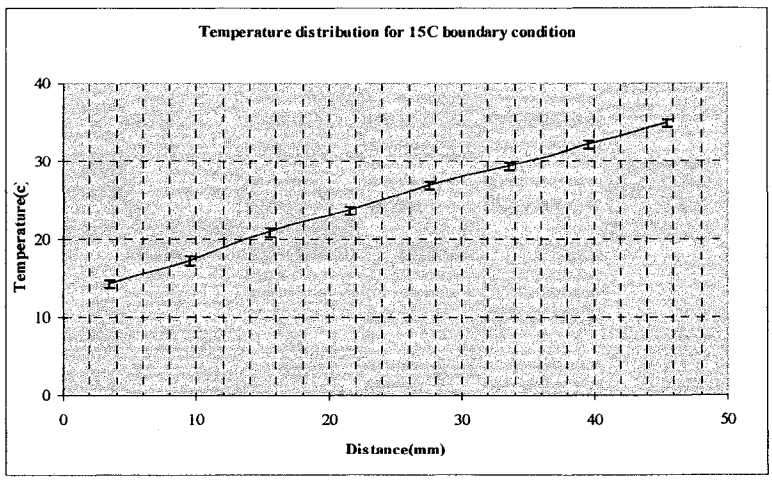

Figure 40. Temperature distribution for glycol at 15^0C boundary condition

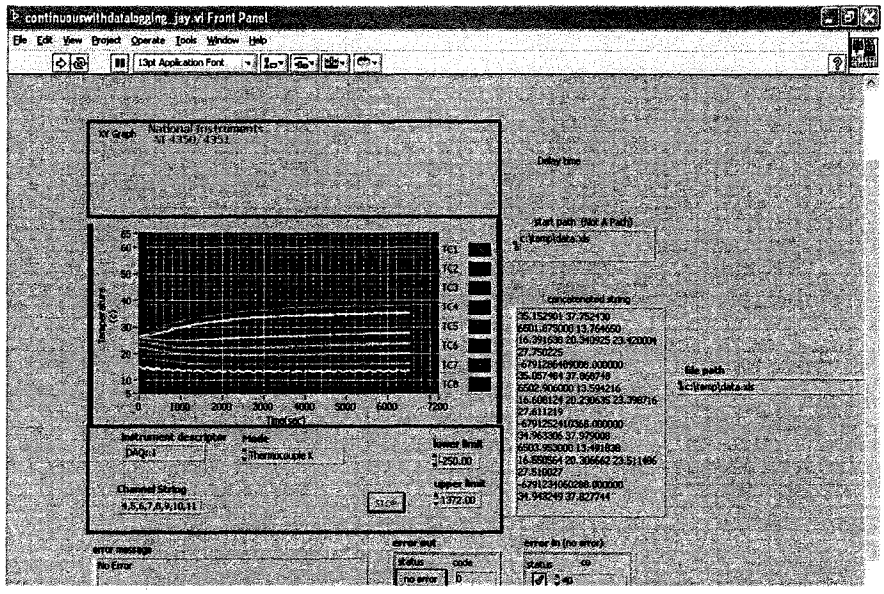

Figure 41. Diagram showing steady state for glycol

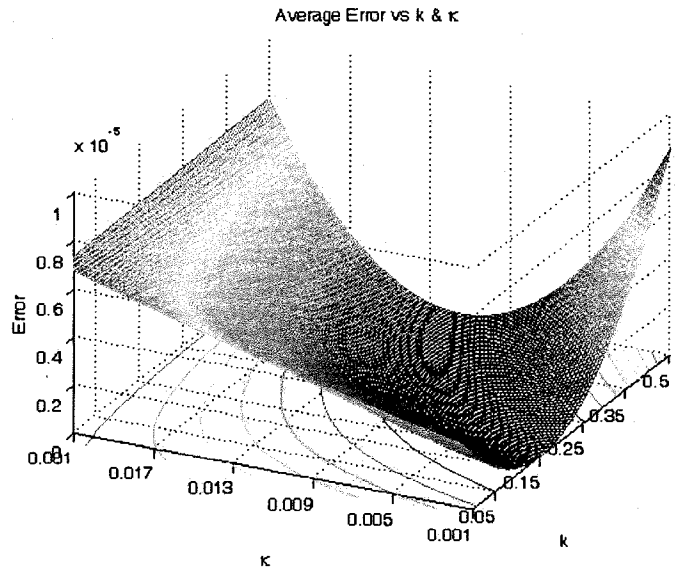

Figure 42. Graph for conductivity and absorption coefficient of Glycol

The optimized values of the two parameters k and κ for Glycol are found to be

k=0.26W/m.K

$\kappa=0.005cm^{-1}$

4.1 Error Estimation in Calculated Result

This section provides some insight into the uncertainty of the calculated values of conductivity and absorption coefficient. In order to accomplish this task each single experimental run is considered for each of the test fluids. The data points which are considered here are obtained from each of the thermocouples after their readings reached steady state for that particular setting of the heat flux imposed condition and the cold plate set temperature. As a sample of the error analysis the data is used for each test fluid having a 15^0C as the cold plate boundary condition and 60W halogen bulb as the heat source. The error in temperature measurement for this particular setting is associated with the error given by thermocouple manufacturer's value. The mean value and the standard deviation for each of the test fluids are calculated.

Standard Deviation

The standard deviation describes the scatter of measurement about the mean value and is given by the following formula (29)

$$s = \frac{\sqrt{\sum (x - \bar{x})^2}}{n-1}$$

The following table gives the values of the standard deviation calculated using above formulae for water.

Water		
Thermocouple No.	Standard Deviation (C)	Average Standard Deviation ($\underline{C}$)
1	1.45	1.54
2	.95	
3	1.24	
4	.86	
5	1.09	
6	1.78	
7	1.45	
8	1.63	

The thermocouple No. 1 is the thermocouple which is near the lower boundary that is near the cold plates and the thermocouple no. 8 is the top most thermocouple in the test section.

The following table gives the values of the standard deviation for Glycerin

Glycerin		
Thermocouple No.	Standard Deviation (C)	Average Standard Deviation ($\underline{C}$)
1	1.02	1.15
2	1.23	
3	.85	
4	.95	
5	1.12	
6	.89	
7	1.25	
8	1.29	

The following table gives the values of the standard deviation for Glycol

Glycol		
Thermocouple No.	Standard Deviation (C)	Average Standard Deviation (C)
1	1.71	1.51
2	1.34	
3	.67	
4	.98	
5	1.18	
6	1.53	
7	1.26	
8	1.31	

The k-type thermocouples that are used in the present experimental work have measurement accuracy in the range of $\pm 1^0$C (www.omega.com). Also the temperature controller that is employed in the set-up to control the cold plate temperature which is used as the lower boundary condition has also accuracy in the range similar to that of thermocouples and that is $\pm 1^0$C (www.americool.com). The error estimation because of the physical values of these two equipments is given in this section. The influence of the uncertainty because of the physical value of these equipments is estimated for thermal conductivity and absorption coefficient. The change in thermal conductivity is given by (Yoshida [14])

$$\Delta k = 100(k_e - k_r / k_r$$

Similarly the absorption coefficient is given by (Yoshida [14])

$$\Delta\kappa = 100(\kappa_e - \kappa_r / \kappa_r$$

Where the subscripts r and e indicate the real value and the value obtained under the given conditions. In order to know the influence of the temperature, the value of the temperature is changed according to the measurement accuracy given by the manufacturer for both thermocouple and the temperature controller and the new values for both coefficients are calculated using the same software that is initially used to estimate radiation absorption coefficient and thermal conductivity. The following table shows the estimated influence of temperature on conductivity and absorption coefficient for each test fluid. For this analysis the experimental values obtained for 60W heat source and 15^0C cold plate boundary condition are used for each fluid.

Factor	Δk	$\Delta\kappa$
Water	±3.15%	±3.67
Glycerin	±4.86%	±4.56%
Glycol	±3.41%	±3.35%

CHAPTER 5

CONCLUSION AND FUTURE WORK

Literature review showed that there is numerous amount of work done for calculation of the thermal properties of semi-transparent liquids. In this work convection heat transfer is not desired because it will not give an accurate estimate of the conductivity. This work is combination of both the experimental and the numerical approach. Compared with previous work the present work is distinguished by the steady state maintained at the boundary level and also by the use of approximation relationship which has not been used frequently. Limited research is carried out for this particular problem with taking into consideration the radiation factor. The objective of the work is mainly associated with the heat transfer process with conduction and radiation modes of heat transfer only. The results that are obtained from both experiments and the code are matching in close proximity with the one given in literature (27). The thermal conductivity of water is found to be 0.64 W/m.k. The factor that plays an important role is the temperature. The results showed the expected dependence of the thermal conductivity and absorption coefficient of water. As the temperature profile changed the values of the two properties also changed. The point that is noted explicitly in this work is that the conductivity and the absorption coefficient values do not change in a great

proportion. This particular observation of the results provides its proof from the fact that the temperature profile in the test section for each liquid and at each boundary condition does not change vaguely. The temperature profile almost remains in close proximity with different set conditions at the lower boundary and the upper boundary. One of the key issues that have been seen in the experimental work and which has been well taken care of is the convection heat transfer. As the arrangement was made in such a manner to avoid the heat transfer by convection. The results for Glycerin show little amount of change in their values of thermal conductivity and the absorption coefficient. (30).As per the literature the absorption coefficient of Glycerin is not stable in visible range (400nm to 700nm); the same result is obtained from the experimental work. The values of the absorption coefficient for Glycerin varied from 0.002 cm^{-1}. Some of the test with glycerin had low thermal conductivity but the temperature profile was increasing significantly. This is because of the higher absorption. This particular phenomenon provides a strong support that though the thermal conductivity of Glycerin is low but because of the absorption coefficient the amount of heat received by Glycerin is higher

Similar results are obtained for Ethylene Glycol. Ethylene Glycol is found to have low thermal conductivity of 0.26W/m.K., and a very low absorption coefficient of the order $0.005cm^{-1}$. This value matches closely with the one from literature (28). The following table gives the values found by other researchers and the range of values obtained during present work. The unit of k in the following table is W/m.K and that of κ is cm^{-1}

	Present work	Literature
I. Water		
k	0.64	0.65
κ	0.5	0.54
II. Glycerin		
k	0.32	0.32
κ	0.002	0.0025
III. Glycol		
k	0.26	0.27
κ	0.005	0.0055

Sources of Errors

During the course of experiments there are few sources of error which can play an important role during the tests. These issues are listed below.

1. Accuracy of the measuring equipments like the thermocouple and the temperature controller. The accuracy of the thermocouple and the temperature controller is $\pm 1^{0}$C.
2. The cold source that is provided to minimize the convection and accuracy of this equipment. The control accuracy of the cold pates is $\pm 1^{0}$C.
3. The surrounding temperature which plays an important role in stabilizing the steady state. Each run almost took 60 to 100 minutes. If there are other processes going on in the same lab or area where the experiment is taking place, then all those factors are accounted for measuring the temperature values. Like if some

heat is added to the area as outcome of some other experiment it would be difficult to maintain the steady state for this system or it may give deviating results in the measurement.

4. The repeatability of the experiments, in some cases repeating the experiment more than once was needed to reduce the fluctuation in measurements. Also if multiple users are allowed to do the same test and then the average of all readings is taken, that would minimize further errors in experiments. This is important because every user will have different way of handling the set-up and that might refine the overall results.

Future Work

The goal of this work is to develop a method to determine the thermal properties of the molten salts where the effects of thermal conductivity are separated from the radiation absorption properties. To conduct this method for higher temperatures and potentially corrosive transparent fluids the experimental setup need to become suitable to handle melting point temperatures of molten salt (454^0C). Proper selection of the crucible materials to handle the corrosiveness issues is another challenge.

NOMENCLATURE

Symbol	Definition
A	Area
C	Velocity of light
c_p	Specific heat at constant pressure
E	Emissive power
E'	Irradiation
$\vec{E}$	Radiant energy flux
E_n	Net radiant energy flux
H	Vertical distance between two plates
h	Enthalpy
I	Intensity of radiation
k	Thermal conductivity
K_{eff}	Effective thermal conductivity
N	Dimensionless parameter
n	Index of refraction
p	Pressure
q''	Heat flux

q'''	Heat generation
U	Velocity outside the boundary layer
t	Time
v	Velocity in y direction
V	Volume
W	Velocity in z direction
W	Work done by the fluid
x	Position coordinate
y	Position coordinate
z	Position coordinate
Greek Symbols	
α	Radiation absorptivity of the surface
β	Radiation extinction coefficient
γ	Scattering function
ε	Radiation emissivity
ζ	Dimensionless independent variable
η	Dimensionless independent variable
θ	Angle between the pencil at rays
κ	Absorption coefficient
λ	Wavelength
μ	Dynamic Viscosity
ρ	Density

σ	Stefan-Boltzmann Constant
τ	Optical thickness
Subscripts	
c	Refers to conduction
r	Radiant
λ	Refers to monochromatic
bb	Black body

REFERENCES

1. ASTM D 2717-95 Standard test method for Thermal Conductivity of Liquids.

2. M Terzic, J Jovanovic-Kurepa and J Slivka. The influence of sample thickness on the determination of large optical absorption coefficients in liquids. Journal of Physics D: Applied Physics 31 (1998) 1368-1374.

3. H Mercier, F Gaillard, J Cariou et J Lotrian. Dual beam pulse experimental setup for measuring attenuation coefficients of liquids: application to distilled water in the 414-662 nm spectral range. Journal of Physics D: Applied Physics, 15 (1982) 563-569.

4. E. McLaughlin. The thermal conductivity of liquids and dense gases. Department of chemical engineering and chemical technology, Imperial College, S. Kensington, London.

5. Walter N Trump, Harold W. Luebke, Lewis Fowler and Edward M. Emery. Rapid measurement of liquid thermal conductivity by the transient hot wire method. Review of Science Instruments, Vol. 48, No.1, January 1977.

6. Y.H.Julia, J.F. Renaud and D.J. Ferrand. Device for automatic thermal conductivity measurements. Review of Science Instruments, Vol.48, No. 12, December 1977.

7. Vincent J. Castelli and Everett M. Stanley. Thermal conductivity of distilled water as a function of pressure and temperature. Journal of Chemical and Engineering Data, Vol.19, No.1, 1974.

8. Y. Kato, K. Kobayasi, N. Araki and F. Furukawa. An accuracy analysis of the thermal diffusivity measurement of molten salts by stepwise heating and improved apparatus. Journal of Physics E: Scientific Instruments 1977 Volume 10

9. D.F. Williams, L.M. Toth, K.T. Clarno. Assessment of candidate molten salt coolants for the advanced high temperature reactor (AHTR). ORNL/TM-2006/12.

10. K.Cornwell. The thermal conductivity of molten salts. Journal of physics D: Applied Physics, 1971, Vol.4.

11. James A. Coakely Jr. An approximate mean absorption coefficient of H_2O. Journal of quantum spectroscopic radiation transfer. Vol. 13, pp. 937-952.

12. C Ould-Lahoucine, S. Sakashita and T. Kumada. A method for measuring thermal conductivity of liquids and powders with a thermistor probe. International communications in heat and mass transfer, Vol. 30, No.4, pp. 445-454, 2003.

13. Ryuzi Yano, Yukio Fukuda and Tsuneo Hashi. Thermal conductivity measurement of water-ethanol solutions by the laser induced transient grating method. Chemical Physics 124 (1988) 315-319.

14. A. Yoshida, T. Fujisaki, H. Tadokoro and S. Washio. Simultaneous measurement of thermo physical and radiative properties of semi-transparent liquids. Fluid phase equlibria 125 (1996) 275-282.

15. C.T. Ewing, J.R. Spann and R. R. Miller. Radiant transfer of heat in molten inorganic compounds at high temperatures. Journal of chemical and engineering data. Vol.7, No. 2, April 1962.

16. Quanfang Lei, Yu-Chun Hou and Ruisen Lin. A new correlation for thermal conductivity of liquids. Chemical engineering science, Vol. 52, No.8, pp 1243-1251, 1997.

17. L.H. Martin and K.C. Lang. The thermal conductivity of water. Physics society, XLV 4.

18. Iosif M. Levin and Kusiel Shifrin. Potential for determining the sea water absorption coefficient by satellite pulsed radar method. Remote sensing of environment, Vol. 65, pp 105-111(1998).

19. R. Viskanta and R.J. Grosh. Heat transfer by simultaneous conduction and radiation in an absorbing medium. Journal of heat transfer. 1962.

20. R. Viskanta. Heat Transfer in thermal radiation absorbing and scattering media. PhD thesis. Purdue University, also ANL 6170, May 1960.

21. C.Y. Ho. Transport properties of fluids. Vol. I-1.1988

22. Frank P. Incropera and David P. Dewitt. Introduction to heat transfer. Third edition.

23. Proposal. Development of advanced high temperature heat exchangers. NSTG website http://nstg.nevada.edu.

24. A. P. Ivanov, I.I. Kalinini, A.I. Kolensik and P.P. Bondarenko. Translated from Zhurnal Prikladnoi, Vol. 29, No. 4, pp 710-716, October 1978

25. Yu. Usmanov, V. Eliseev and G.Ya. Umarov. The optical characteristics of a solar pond. Geliotekhnika, Vol. 7, No. 3, pp 78-81, 1971

26. Hale, Querry. Optical constants of water. Journal of applied Optics, 12, 555, 1973.

27. Segelstein. The complex refractive index of water. Compendium of optical absorption of water.1981.

28. C. Jacinto. High sensitivity absorption coefficients measurements. Journal of physics. IV France. 2125(2005).229-232

29. W.G.Woods. Experimental methods.1974.

30. M. Cheikh, H.L. Nghiem. Time resolve diffusive wave spectroscopy.

31. Komarov, S.V. Sano. Heat transfer in preheated in liquid bath. ISIJ International, V 38, n 10, 1998, p 1045-105.

32. Rolf. E. Hummel. Handbook of optical properties. Volume 1. 1995.

APPENDIX

The Mat Lab Code

The call function

```
**************************************************************************

unction f = cond(T);

global capa k zeta1 n sigma1 T0 Th


a=(T0*(1-zeta1))+(Th*zeta1);

b=((4*n^2*sigma1)/(3*capa*k));

c=b*(((T0^4)*(1-zeta1))+((Th^4)*zeta1));


%Function y

f = T + b*(T^4)-a-c;

**************************************************************************

global capa zeta1 n sigma1 T0 Th k


%Setting the parameters


T1=279; % Deg K

n=1; % constant

sigma1=5.670e-8; %1.714e-9; Wm-2K-4
```

```
% T0=278; % deg K
% Th=350; % deg K

zeta=[0.0045,0.0105,0.0165,0.0225,0.0285,0.0345,0.0405,0.0465]/0.05;
Texpar=[279.47,282.99,287.37,290.49,294.44,301.23,304.12,307.95];
zeta=[0.07,0.19,0.31,0.43,0.55,0.67,0.79,0.91];
%zeta=[0.19,0.31,0.43,0.55,0.67,0.79];
Texpar=[279.876498,283.267362,287.345264,291.1003,296.050106,300.794136,306.476
788,313.017761];
%Texpar=[283.267362,287.345264,291.1003,296.050106,300.794136,306.476788];

% Generating arrays of k and kappa
kvar=linspace(0.20,0.27,20); mm=length(kvar);
caar=linspace(0.003,0.007,20); ll=length(caar);
% 2.1845e+014
kvar=linspace(0.05, 1.4, 100); mm=length(kvar);
caar=linspace(0.05, 1.4, 100); ll=length(caar);


T0 = Texpar(1);
Th = Texpar(length(Texpar));
T0 = 278;
```

```
Th = 315;

%Calling the function fzero

% solve for T(k,capa,zeta), error(k,capa,zeta) and comparing with
% experimental values
   options = optimset('Tolfun', 1e-6);
   for i=1:mm
      k=kvar(i);
      for j=1:ll
      capa=caar(j);
zeta1=zeta(8);
      Texp1=Texpar(8);
      T1 = Texp1;
      myT8(i,j) = fzero(@cond_fake,T1,options);
      error8(i,j)=((myT8(i,j)-Texp1)/myT8(i,j))^2;
      err(i,j) = error8(i,j);

      cappa = 0;
      T1 = 0;
      zeta1 = 0;

      end
```

```
    k = 0;
  end

% subplot(3,3,2), meshc(kvar,caar,error2)
% subplot(3,3,3), meshc(kvar,caar,error3)
% subplot(3,3,4), meshc(kvar,caar,error4)
% subplot(3,3,5), meshc(kvar,caar,error5)
% subplot(3,3,6), meshc(kvar,caar,error6)
% subplot(3,3,7), meshc(kvar,caar,error7)
% subplot(3,3,8), meshc(kvar,caar,error8)

% for k=8:size(err,3)
% %subplot(3,3,k),
% figure
% meshc(kvar,caar,err(:,:,k));
% set(gca,'XLim',[kvar(1), kvar(length(kvar))]);
% set(gca,'YLim',[caar(1), caar(length(caar))]);
% grid on
% xlabel('k'); ylabel('\kappa'); zlabel('Error');
% title([{'Error vs k & \kappa'}, {['\zeta = ', num2str(zeta(k))]}]); %, {['\zeta = ',
num2str(zeta(k))]}]);
% end
```

```
figure
plot(kvar, mean(err(:,:)), 'b.-');
xlabel('k'); ylabel('Error');
grid on
title('Average Error vs k');

figure
plot(caar, mean(transpose(err(:,:))), 'b.-');
xlabel('\kappa'); ylabel('Error');
grid on
title('Average Error vs \kappa');
```

VITA

Graduate College
University of Nevada, Las Vegas

Jayant Prabhakar Patil

Home Address:
1455 East Rochelle Avenue, Apt#4
Las Vegas, NV 89119

Degrees:
Bachelor of Engineering, Mechanical Engineering, 2002
Badnera Engineering College, Amravati University, India

Thesis Title:
Determining Thermal Conductivity And Absorption Coefficient Of Semi-Transparent Liquids Using Numerical And Experimental Approach

Thesis Examination Committee:
Chairperson, Dr. Samir Moujaes., Ph. D., PE
Committee Member, Dr. Anthony Hechanova, Ph. D.
Committee Member, Dr. Mohamed Trabia, Ph. D.
Graduate Faculty Representative, Dr. Mohamed Kaseko, Ph. D.